Molecular Biology of the Cell
Vol. 17, 3729–3744, September 2006

Phosphoinositide 3-Kinase C2β Regulates Cytoskeletal Organization and Cell Migration via Rac-dependent Mechanisms[D] [V]

Roy M. Katso,*† Olivier E. Pardo,‡ Andrea Palamidessi,§ Clemens M. Franz,* Marin Marinov,‖ Angela De Laurentiis,‖ Julian Downward,‡ Giorgio Scita,§ Anne J. Ridley,*¶ Michael D. Waterfield,*¶ and Alexandre Arcaro‖

*Ludwig Institute for Cancer Research, Royal Free and University College Hospital Medical School, London W1W 7BS, United Kingdom; ‡CRUK London Research Institute, London WC2A 3PX, United Kingdom; §European Institute of Oncology, The FIRC Institute for Molecular Oncology, 20139 Milano, Italy; ‖Division of Clinical Chemistry and Biochemistry, University Children's Hospital Zurich, CH-8032 Zurich, Switzerland; and ¶Department of Biochemistry and Molecular Biology, University College London, London WC1E 6BT, United Kingdom

Submitted November 28, 2005; Revised May 22, 2006; Accepted June 7, 2006
Monitoring Editor: Richard Assoian

Receptor-linked class I phosphoinositide 3-kinases (PI3Ks) induce assembly of signal transduction complexes through protein–protein and protein–lipid interactions that mediate cell proliferation, survival, and migration. Although class II PI3Ks have the potential to make the same phosphoinositides as class I PI3Ks, their precise cellular role is currently unclear. In this report, we demonstrate that class II phosphoinositide 3-kinase C2β (PI3KC2β) associates with the Eps8/Abi1/Sos1 complex and is recruited to the EGF receptor as part of a multiprotein signaling complex also involving Shc and Grb2. Increased expression of PI3KC2β stimulated Rac activity in A-431 epidermoid carcinoma cells, resulting in enhanced membrane ruffling and migration speed of the cells. Conversely, expression of dominant negative PI3KC2β reduced Rac activity, membrane ruffling, and cell migration. Moreover, PI3KC2β-overexpressing cells were protected from anoikis and displayed enhanced proliferation, independently of Rac function. Taken together, these findings suggest that PI3KC2β regulates the migration and survival of human tumor cells by distinct molecular mechanisms.

INTRODUCTION

Phosphoinositide 3-kinases (PI3Ks) trigger activation of signaling pathways in response to extracellular stimuli that regulate diverse cellular programs such as cell survival, proliferation and migration, phagocytosis, and glucose homeostasis (Katso *et al.*, 2001). There are three classes of PI3Ks in mammals. Class I PI3Ks primarily generate PI(3,4,5)P_3, which binds to pleckstrin homology (PH) domains and activates a variety of proteins including the serine/threonine kinase PKB/Akt and exchange factors for small GTPases. Class II PI3Ks have the potential to generate PI(3,4,5)P3, but the type of PIPs that they produce in vivo has not been fully characterized. The sole class III PI3K, Vps34, produces PI(3)P. Class I PI3Ks and 3-phosphophorylated phosphatidylinsitols (PIs) have been implicated in cancer: the phosphatase PTEN removes the 3-phosphate from 3-phosphorylated inositides generated by PI3Ks, and PTEN is a tumor suppressor gene mutated in a variety of human cancers (Yamada and Araki, 2001). In addition, mutation, amplication and/or overexpression of some PI3K class I catalytic subunits has been found is some cancers (Katso *et al.*, 2001; Vogelstein and Kinzler, 2004).

Although the class I PI3K family has been implicated in multiple cellular processes (Katso *et al.*, 2001; Vanhaesebroeck *et al.*, 2001), much less is known about the function of the class II PI3K enzymes, PI3KC2α, PI3KC2β, and PI3KC2γ. Both PI3KC2α and PI3KC2β have been implicated in signaling by tyrosine kinase receptors. They are recruited to a signaling complex including the EGF receptor after EGF activation of A-431 cells (Arcaro *et al.*, 2000) and to the stem cell factor (SCF) receptor in small lung cell carcinoma cell lines (Arcaro *et al.*, 2002). The interaction of PI3KC2β with the EGF receptor requires the adaptor protein Grb2, and the SH3 domains of Grb2 bind directly to three proline-rich regions near the amino terminus of PI3KC2β (Wheeler and Domin, 2001). Interestingly, PI3KC2β is required together

This article was published online ahead of print in *MBC in Press* (http://www.molbiolcell.org/cgi/doi/10.1091/mbc.E05–11–1083) on June 14, 2006.

[D] [V] The online version of this article contains supplemental material at *MBC Online* (http://www.molbiolcell.org).

† Present address: Systems Research, GlaxoSmithKline Pharmaceuticals, Gunnels Wood Road, Stevenage, SG 2N1 Hertfordshire, United Kingdom.

Address correspondence to: Alexandre Arcaro (Alexandre.Arcaro@kispi.unizh.ch).

Abbreviations used: EGFR, epidermal growth factor receptor; Erk, extracellular signal-regulated kinase; F-actin, filamentous actin; MEK, mitogen-activated Erk kinase; JNK, c-Jun N-terminal kinase; mTOR, mammalian target of rapamycin; PH, pleckstrin homology; PI, phosphatidylinositol; PI3K, phosphoinositide 3-kinase; PKB, protein kinase B; pY, phosphotyrosine; SCF, stem cell factor; SCLC, small cell lung cancer; SH, Src homology.

with class I_A PI3Ks for activation of Akt by SCF (Arcaro *et al.*, 2002).

To investigate signaling by PI3KC2β, we sought to identify its interacting partners. We identified Eps8 as a tyrosine-phosphorylated protein associated with PI3KC2β and established that PI3KC2β is part of a multiprotein signaling complex including Grb2, Eps8, Abi1, and Sos that is assembled and recruited to the EGF receptor, after EGF stimulation. PI3KC2β regulated Rac activity and c-Jun N-terminal kinase (JNK) activation, consistent with the role of the Eps8-Abi1-Sos complex as an exchange factor for Rac. As a result, PI3KC2β expression enhanced membrane ruffling and cell motility. Moreover, PI3KC2β-expressing cells displayed reduced sensitivity to detachment-induced apoptosis and increased proliferation, which involved a Rac-independent signaling pathway.

MATERIALS AND METHODS

Antibodies and Reagents

The following antibodies were used: Akt, Sos1, 9E10 myc epitope, and phospho-Erk (Santa Cruz Biotechnology, Santa Cruz, CA), phosphor-Akt (Ser473), Jun, phospho-Jun, JNK, and phospho-JNK (New England Biolabs, Beverly, MA), Grb2 monoclonal and polyclonal, Shc, Eps8, E-cadherin and pan-Erk antibodies (Transduction Laboratories, Lexington, KY), Rac, and 4G10 anti-phosphotyrosine (Upstate Biotechnology, Lake Placid, NY), E-cadherin monoclonal antibody (mAb; Zymed Laboratories, South San Francisco, CA).

The rabbit antibody to Abi1 was a kind gift from Paolo Di Fiore (European Institute of Oncology, Milan, Italy). Recombinant human EGF was purchased from R&D Systems (Minneapolis, MN). TRITC-conjugated phalloidin was obtained from Sigma-Aldrich (St. Louis, MO). The Akt inhibitor (1L-6-hydroxymethyl-chiro-inositol 2-(R)-2-*O*-methyl-3-*O*-octadecylcarbonate), the JNK inhibitor I, PD098059, and SB202190 were purchased from Calbiochem (La Jolla, CA).

Cell Lines

A-431 cell lines stably expressing PI3KC2β WT and DN were generated as previously described (Arcaro *et al.*, 2000). The A-431 human epidermoid carcinoma cells were maintained at 37°C, 10% CO_2 under humidified conditions in DMEM supplemented with 10% fetal bovine serum (FBS), penicillin-streptomycin, and glutamine. The stock cell cultures were passaged every 4 d. Cells were made quiescent by switching them to DMEM supplemented with 0.1% fetal calf serum (FCS) for 24 h. HEK 293 cells were maintained in DMEM/10% FCS.

Immunoprecipitation and Immunoblotting Analysis

Cells were grown to 80% confluence in 10-cm dishes and starved for 24 h in DMEM supplemented with 0.1% FCS. Where indicated, cells were then stimulated with 1 nM EGF (6 ng/ml) for the indicated time periods. The cells were washed once with ice cold phosphate-buffered saline (PBS) before lysis on ice for 30 min in 1.00 ml of lysis buffer (1% Triton X-100, 0.5% NP-40, 150 mM NaCl, 50 mM Tris.HCl, pH 7.4, 1 mM EDTA, 0.5 mM EGTA) supplemented with protease inhibitors (10 μg/ml aprotinin, leupeptin, pepstatin A, trypsin, and 100 μg/ml phenylmethylsulfonyl fluoride) and phosphatase inhibitors (Sigma phosphatase cocktail I and II solutions). Insoluble material was removed by centrifugation for 30 min (15,000 rpm at 4°C). The Triton-insoluble fraction was analyzed by reextraction of the pellet from above in RIPA lysis buffer (1% Triton X-100, 50 mM Tris.Cl, pH 7.4, 150 mM NaCl, 1 mM EDTA, 1% sodium deoxycholate, 0.1% SDS, 1 mM sodium orthovanadate, 25 mM sodium fluoride, supplemented with 100 mg/ml AEBSF, and 5 mg/ml each of leupeptin, pepstatin A, and aprotinin). The lysates were equalized for protein content before being immunoprecipitated. The total protein concentration was measured using the calorimetric BCA protein assay (Pierce, Rockford, IL). Protein, 800 μg, was incubated with the respective antibodies preadsorbed onto 50 μl of protein A or G agarose beads. After 4-h incubation at 4°C, the immune-complexes were washed three times in ice-cold cell lysis buffer supplemented with 500 mM NaCl and protease inhibitors. The immune-complexes were eluted and denatured by boiling for 5 min in SDS sample buffer (50 mM Tris.HCl, pH 6.8, 2% SDS, 10% glycerol, 5% β-mercaptoethanol, and 0.25% bromophenol blue). For analysis of total cell lysates, 40 μg of total protein was resolved on 20-cm Hoeffer SDS-PAGE gels (8–12%) and transferred to PVDF membranes in a Tris-glycine-methanol buffer (190 mM glycine, 20% methanol, 25 mM Tris.HCl, pH 7.4) at 150 mA per gel for 7 h at room temperature. After the transfer, blots were processed with the respective antibodies using standard immunoblotting procedures.

Peptide Coupling and Affinity Purification

Peptides were purified by high-pressure liquid chromatography and lyophilized (Alta Bioscience, Birmingham, United Kingdom). The epidermal growth factor receptor (EGFR) peptides and their phosphorylated (p) derivatives corresponding to the EGFR pY992 Shc (DDVVDADEYLIP/DDVVDADEpYLIP) and pY1068 Grb2 (DTFLPVPEYINQ/DTFLPVPEpYING) Src homology 2 (SH2) docking sites were used in the peptide pulldown experiments. The PI3KC2β N-terminal proline-rich peptides, proline-rich peptide (PR) 1 SPPPLPPRAS, PR2 WDTPPLPPRK, and PR3 MPPQVPPRTY were used to map the putative Grb2 SH3-binding site. The lyophilized peptides were resuspended in a sodium phosphate buffer solution (0.1 M sodium phosphate, 150 mM NaCl, pH 7.4, solution). Peptides were immobilized to Actigel-ALD resin (Sterogene Bioseparations, Arcadia, CA) according to manufacturer's instructions. Aliquots of coupled peptides were stored at 4°C in the sodium phosphate buffer supplemented with phosphatase inhibitors and 0.01% sodium azide. For the peptide pulldowns, 1 μg of coupled peptide was incubated with 800 μg of protein at 4°C on a rotating wheel for 1 h. The peptides were washed four times in lysis buffer before subjecting the complexes to SDS-PAGE and immunoblot analysis.

Production of GST-Fusion Proteins

pGEX-2T expression vectors encoding PI3KC2β N-terminal (amino acids 1–300) domain, N-terminal Grb2 SH3 domain, C-terminal Grb2 SH3 domain, Abi1 SH3 domain, Raf Ras-binding domain, and PAK CRIB domain were transformed into *Escherichia coli* BL21 cells. GST fusion protein expression was induced by adding 1 mM IPTG to a 1-l culture of exponentially growing cells at 30°C for 4 h. The bacterial cells were harvested by centrifugation and were either immediately processed or frozen down as bacterial pellets at −70°C. The bacterial pellets were lysed at 4°C in 50 mM Tris.Cl, pH 8.0, 2 mM $MgCl_2$, 10% glycerol, 20% sucrose, 2 mM DTT, 100 μg/ml AEBSF, 1 μg/ml each of aprotinin, leupeptin, and pepstatin A. GST fusion proteins were affinity-purified by incubating the clarified lysate with glutathione Sepharose beads (Pharmacia Biotech, St Albans, United Kingdom) at 4°C on a rotating wheel for 1 h. After extensive washing of the Sepharose beads, bound proteins were eluted by incubating the glutathione Sepharose with 10 mM reduced glutathione in 50 mM Tris.Cl, pH 8.0. The eluted proteins were dialyzed with 100 mM Tris.HCl, pH 7.4, 150 mM NaCl and stored in aliquots in a buffer made up of 20% glycerol, 100 mM Tris.Cl, pH 7.4, and 150 mM NaCl at −70°C.

Rac Activity Assays

A glutathione *S*-transferase (GST)-PAK Cdc42 and Rac-binding region (CRIB) fusion protein was incubated with cell lysates to pull down GTP-bound active Rac. GST-PAK CRIB fusion protein was prepared just before the pulldown assays. (This is all in the section above.) The Sepharose beads with bound GST-PAK CRIB were washed three times in lysis buffer and once in Rac pulldown buffer (50 mM Tris.HCl, pH 7.4, 12 mM $MgCl_2$, 10% glycerol, 100 mM NaCl, 1% NP-40, 50 mM NaF, 1 mM sodium orthovanadate, 1 μg/ml pepstatin, 1 μg/ml aprotinin, 1 μg/ml leupeptin, and 100 μg/ml AEBSF). The Sepharose beads were aliquoted (25 μl) into individual tubes for the Rac pulldown assay. Alternatively, GST-PAK CRIB beads were purchased from Upstate Biotechnology. A-431 cells were grown to 80% confluence and made quiescent by culturing them in serum-free medium (0.1%) for 24 h. The cell culture plates were immediately placed on ice, washed once with ice-cold PBS, and lysed for 5 min on ice with 1 ml Rac pulldown buffer (this is given above). The lysates were clarified by centrifugation (14,000 × *g*, 4°C, 5 min), and protein concentration was determined (Bradford assay, Pierce). Equal amounts of lysates were incubated with GST-PAK CRIB fusion protein at 4°C for 30 min. The beads were washed three times in lysis buffer and eluted in Laemmli sample buffer. The amount of Rac pulled down was determined by immunoblotting with anti-Rac mAb (Upstate Biotechnology).

PI3K Assays

For the immune-complex kinase assays, cells were lysed in RIPA buffer for 30 min on ice. The cell lysates were clarified by centrifugation (14,000 × *g*, 4°C, 15 min), and aliquots were taken from the respective tubes for protein quantification. Equal amounts of lysates were incubated with the respective antibodies for 4 h at 4°C. The immune-complexes were washed three times in lysis buffer, once in 50 mM HEPES, pH 7.5, and once in 2× PI3K assay buffer (40 mM Tris.HCl, pH 7.4, 200 mM NaCl). The PI3K assay was initiated by resuspending the immune-complexes in 25 μl of 2× PI3K assay buffer. The phospholipids (PI, PI(4)P, and PI(4,5)P_2) were sonicated for 10 min and added at a final concentration of 0.2 mg/ml to the sample tubes. The tubes were incubated on ice for 20 min to allow the substrate to bind to the enzyme. Fifteen microliters of the assay reaction mix (40 mM ATP, 3.5 mM divalent cation, and 10 μCi [γ-^{32}P]ATP) were added to each of the sample tubes on ice before transferring them to room temperature for 20 min. The reactions were terminated by placing the tubes on ice and adding 100 μl of 1 M HCl in addition to 200 μl of a 1:1 solution of chloroform and methanol. The samples were vortexed and centrifuged for 2 min at room temperature. The organic phase was collected and extracted with 80 μl of a 1:1 solution of methanol and 1 M HCl. The tubes were vortexed and centrifuged for 2 min at room

temperature, and the organic phase containing the lipids was transferred to a fresh tube. The lipids were dried down in a speed vacuum before determining the amount of radioactivity incorporated by Cerenkov counting. The lipids were resuspended in 30 μl of a 4:1 solution of chloroform and methanol and spotted onto channeled Silica Gel 60 TLC plates (Whatman, Clifton, NJ) that had been pretreated in 1% oxalic acid, 1 mM EDTA, 40% methanol and baked for 15 min at 110°C. The TLC plates were developed in propan-1-ol, 2 M acetic acid (65:35) for 4 h, and the radiolabeled spots were quantified using a PhosphoImager (Molecular Dynamics, Sunnyvale, CA).

Immunofluorescence and Localization of F-Actin

A-431 cells (1×10^4) were seeded on glass coverslips and grown for 48 h. Coverslips were rinsed in PBS and fixed for 10 min in 4% (wt/vol) paraformaldehyde at room temperature. Cells were permeabilized in a solution of 0.2% Triton X-100 for 5 min and then rinsed with PBS. The coverslips were then incubated with either mouse anti-myc epitope (9E10) or anti-E-cadherin antibodies followed by FITC-labeled goat anti-mouse antibodies and TRITC-conjugated phalloidin for 30 min. Coverslips were mounted in Moviol (Calbiochem, San Diego, CA). Cells were examined by confocal laser scanning microscopy (LSM 510; Zeiss, Welwyn Garden City, United Kingdom). Image files were collected as a matrix of 1024 × 1024 pixels describing the average of eight frames scanned at 0.062 Hz.

Transfections

Control and PI3KC2β-transfected A-431 cells were plated on gelatin-coated 13-mm glass coverslips. Cells were transfected with HA-RacN17 or the appropriate empty vector using Fugene 6 (Roche, Lewes, East Sussex, United Kingdom), according to manufacturer's instruction. After 8 h, cells were serum starved in 0.5% FBS overnight, and treated with EGF (100 ng/ml) for 10 min or were mock-treated. Cells were then fixed with 4% paraformaldehyde, permeabilized with 0.1% Triton X-100, and blocked in 1% BSA. Immunostaining was performed with the indicated antibodies. FITC-conjugated goat anti-mouse IgGs were used as secondary antibodies. Each experiment was performed at least there time with similar results.

Time-Lapse Video

Control and PI3KC2β-transfected A-431 cells were plated on 100-mm plates in DMEM containing 10% FBS. For live imaging, cells were analyzed with an Olympus IX-70 (Lake Success, NY), collecting images every 30 s for up to 30 min. Images were compiled into movies by using the program Metamorph.

Cell Proliferation

A-431 cell lines (10^5/ml) were grown for 3 d in serum-containing medium (1 or 10%) in the presence or absence of inhibitors. Cell proliferation was analyzed by MTS assay using the CellTiter 96 Aqueous One Solution Cell Proliferation Assay (Promega, Madison, WI).

Induction of Cell Death by Anoikis

Cells grown in attachment were trypsinized and washed once in E4/10% FCS. The cells were then placed in Ultralow attachment plates (Corning; rehydrated according to manufacturer's instruction) at 1×10^6 cells in 3 ml of E4 medium containing 10% FCS and left for 6, 12, or 24 h at 37°C/10% CO_2 in the presence or absence of 50 μM PD098059 or 10 μM SB202190.

Sub-G1 Determination by Flow Cytometry

In E4 medium, 1×10^6 cells containing 10% FCS were centrifuged at 1000 rpm for 5 min and then washed once in PBS before fixation in ice-cold 70% ethanol for 30 min at 4°C. Cells were then washed twice in phosphate-citrate buffer (198 parts of 0.2 M Na_2HPO_4 and 8 parts of 0.1 M citric acid, pH 7.8), and the pellet was resuspended in 50 μl of 100 μg/ml RNAse for 10 min. DNA content was then determined by flow cytometry after addition of 200 μl of 50 μg/ml propidium iodide (Molecular Probes, Eugene, OR).

Annexin V/Propidium Iodide Flow Cytometry Analysis

Cells were resuspended at 1×10^6 cells/ml in binding buffer (10 mM HEPES, pH 7.4, 140 mM NaCl, 2.5 mM $CaCl_2$). This suspension, 100 μl, was mixed with 5 μl of fluorescein isothiocyanate-conjugated annexin V reagent (Molecular Probes) and 10 μl of propidium iodide solution (Molecular Probes). The samples were left for 15 min at room temperature in the dark before the addition of a further 400 μl of binding buffer. The samples were analyzed by flow cytometry.

Protein Down-Regulation by RNAi Oligonucleotides

All oligonucleotides were purchased from Dharmacon (Boulder, CO) and used at 70 nM. Cells at 50% confluence were transfected using the Oligofectamine transfection reagent (Invitrogen, Carlsbad, CA) according to the manufacturer's instructions. Cells were then incubated at 37°C/10% CO_2 for 48 h to allow for target down-regulation. The efficiency of protein down-regulation was assessed by SDS-PAGE and Western blotting.

E-Cadherin Neutralization

In a normal or ultralow attachment 96-well plates (Corning Glass, Corning, NY), 10^4 cells per well were treated for 12 or 24 h with 20 μg/ml E-cadherin antibody (clone HECD-1, Zymed, South San Francisco, CA) in E4 medium containing 10% FCS. Cells were either analyzed for sub-G1 by flow cytometry or stained for actin using AlexaFluor 488-Phalloidin (Molecular Probes) according to manufacturer's instructions.

Cell Motility Assays

Cells plated at 25% confluence in 24 well-plates were imaged by phase contrast using a motorized-staged environment controlled Zeiss microscope. Time-lapse images (1 image/10 min/well for 18 h) were acquired using a prior camera linked to the AQM Advance 6 Software (Kinetic Imaging, Liverpool, United Kingdom). Each condition was performed in quadruplicate. Fifteen cells were tracked per replicate using a Kinetic Imaging plug-in and tracks analyzed by Mathematica 5 (Wolfram Research, Champaign, IL) for migration speed and persistence distribution.

RESULTS

PI3KC2β Is Associated with Shc and Grb2

To investigate signaling partners of PI3KC2β, we sought to identify PI3KC2β binding proteins. We have previously shown that PI3KC2β associates with a complex of tyrosine phosphorylated proteins that include EGFR-1 in cells stimulated with EGF (Arcaro *et al.*, 2000). A-431 cells expressing Myc-tagged wild-type PI3KC2β (A-431-C2β WT cells) were stimulated with EGF and lysed, and anti-Myc immunoprecipitates from the Triton-soluble and -insoluble fractions were analyzed for the presence of tyrosine-phosphorylated proteins. In the Triton-soluble fraction, two tyrosine-phosphorylated proteins of about 50 kDa were identified by immunoblotting as the p46/p52 Shc isoforms (Figure 1A). In the immunoprecipitates from the Triton-insoluble fraction, in addition to the p46/p52Shc isoforms, p66Shc was also specifically tyrosine phosphorylated (Figure 1B).

Given that the PI3KC2β N-terminal proline-rich domain mediates the interaction of PI3KC2β with Grb2 (Wheeler and Domin, 2001), we tested whether this domain was also responsible for PI3KC2β interaction with Shc. The N-terminal 300 amino acids of PI3KC2β pulled down both Grb2 and Shc (Figure 1, C and D). The interaction between the p66Shc isoform and the PI3KC2β N-terminal region was constitutive, whereas in the case of the p46/p52Shc isoforms it was induced by EGF (Figure 1C). There was an apparent discrepancy between the constitutive association of the PI3KC2β N-terminal region with p66Shc (Figure 1C) and the EGF-stimulated interaction of PI3KC2β with Shc isoforms (Figure 1, B and G). A possible explanation for these differences may be that the PI3KC2β N-terminal region is not accessible in the full-length enzyme before EGF stimulation, whereas in the pulldown experiments (Figure 1C) the recombinant N-terminal region is free to associate with multiprotein complexes involving p66Shc. Both the isolated N- and C-terminal SH3 domains of Grb2 bound PI3KC2β, but not PI3KC2α (Figure 1E), suggesting a Grb2-PI3KC2β isoform-specific interaction. The PI3KC2β domain that binds to Grb2 was mapped through peptide pulldown assays to two proline-rich stretches encompassing proline region 1 (PR1) (SPPPLPPRAS), and PR3 (MPPQVPPRT; Figure 1F). Interestingly, neither of these proline-rich regions is present in the PI3KC2α and γ enzymes, implying that this association may be unique to the β isoform. Coimmunoprecipitation analysis showed that the association between Grb2 and PI3KC2β was constitutive, whereas the interaction between the p46/p52Shc isoforms and PI3KC2β was EGF-dependent (Figure 1G). These results suggest that PI3KC2β is recruited to the EGFR-1 either indirectly through Grb2 interaction with Shc or directly through Grb2 interaction with the EGFR-1. Consistent with

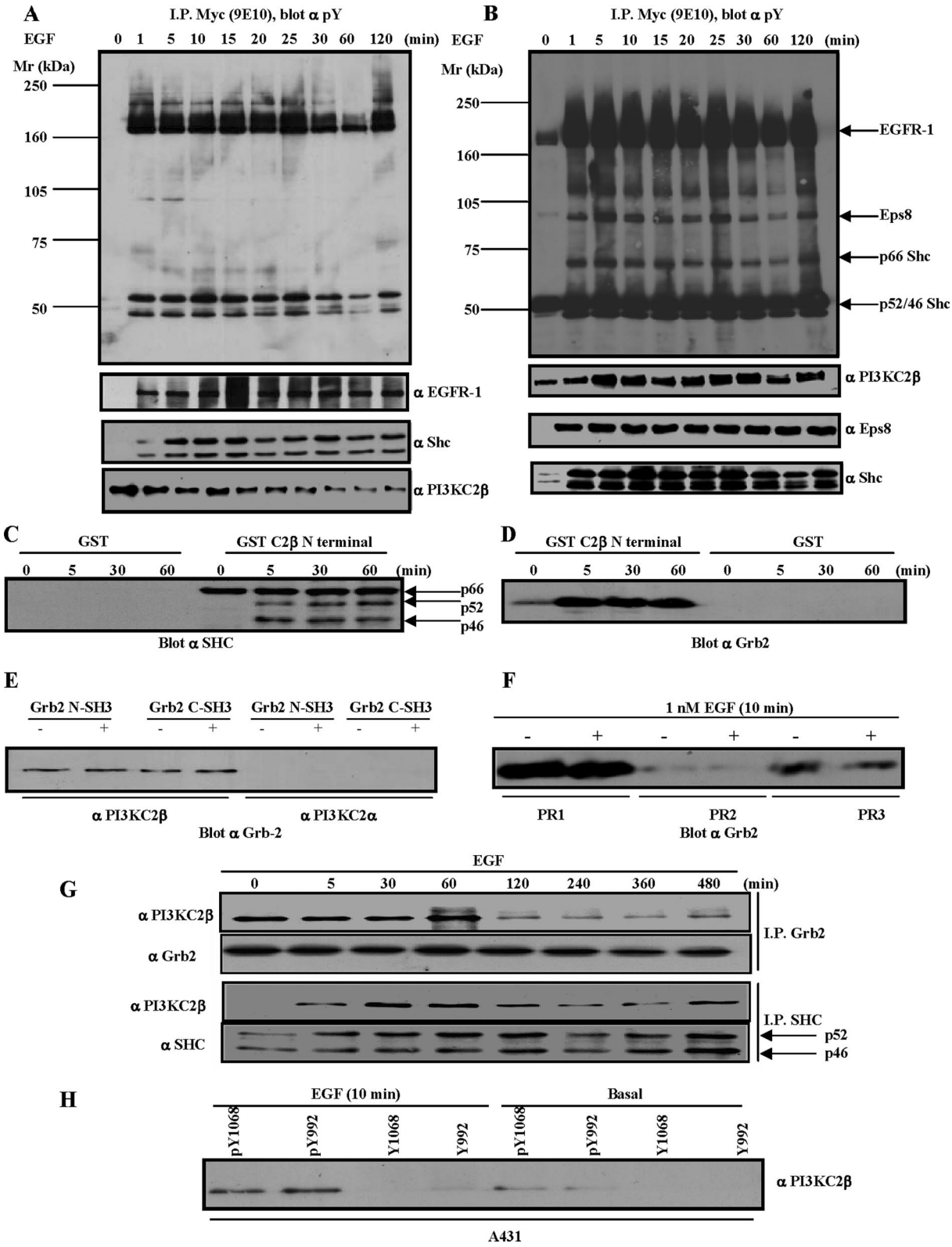

Figure 1. Identification of PI3KC2β-binding proteins. (A) A-431-C2β WT cells were grown to 80% confluence and serum-starved for 24 h before stimulation with EGF for the times indicated. The Triton X-100–soluble (A) and –insoluble fraction (B) were generated as outlined in *Materials and Methods*. PI3KC2β-associated proteins were identified by immunoblotting with the indicated antibodies. (C–E) Lysates from parental A-431 cells were equalized for protein content before immunoprecipitation with the indicated GST-fusion proteins. PI3KC2β N-terminal 300 amino acid domain mediates recruitment of Shc and Grb2 (C and D). Gst-Grb2 pulldowns indicate selective recruitment of PI3KC2β (E). (F) A-431 cell lysates were equalized for protein content before immunoprecipitations with the Actigel coupled PI3KC2β proline-rich peptides, PR1, PR2, and PR3. The amount of Grb2 precipitated by the respective peptides was determined by imuunoblotting.

this hypothesis, EGFR-1 tyrosine-phosphorylated peptides representing residues Y992 and Y1068, the Shc and Grb2 docking sites respectively, immunoprecipitated endogenous PI3KC2β in vitro (Figure 1H).

These observations are in agreement with previous findings that implicated pY992 and pY1068 and Grb2 in the recruitment of PI3KC2β by EGFR-1 (Arcaro *et al.*, 2000; Wheeler and Domin, 2001).

Interaction of PI3KC2β and the Eps8-Abi1-Sos1 Complex

EGF induced a shift in PI3KC2β localization from the Triton-soluble to the -insoluble fraction (Figure 1A, bottom, and B), suggesting an increased association of PI3KC2β with the cytoskeleton and/or signaling microdomains such as rafts. A 98-kDa tyrosine-phosphorylated protein was detected in PI3KC2β immunoprecipitates from the Triton-insoluble fraction and was identified as Eps8 by immunoblotting (Figure 1B). Endogenous Eps8 coprecipitated with PI3KC2β from A-431-C2β WT cells in the insoluble fraction (Figure 1B) and the soluble fraction (Figure 2D). Eps8 has been implicated in the coordination of EGF receptor signaling and trafficking through regulation of Rac and Rab5, respectively, through two mutually exclusive complexes: the Rac GEF ternary complex, Eps8-Abi1-Sos1, and the Rab5-regulatory complex, Eps8-RN-tre (Scita *et al*., 1999; Lanzetti *et al*., 2000). PI3KC2β immunoprecipitates prepared from the Triton-insoluble fraction contained Sos-1 and Eps8 (Figure 2A), and Eps8 immunoprecipitates contained PI3KC2β and Abi1 (Figure 2B), indicating that PI3KC2β is complexed with the Eps8 Rac GEF ternary complex (Figure 2B). A-431 cells normally express low but detectable levels of PI3KC2β (Arcaro *et al.*, 2000). Because of the low levels of endogenous PI3KC2β, we were unable to detect the complex in A-431 cells, but we did detect an association of endogenous Eps8 and PI3KC2β in HEK 293 cells, demonstrating that this is a physiological relevant complex (Figure 2C). In contrast, no association between PI3KC2α and Eps8 was observed in HEK 293 cells. Control immunoprecipitations were also performed, which revealed the specificity of the association of Grb2, Shc, Eps8, and Sos-1 with PI3KC2β in A-431-C2β WT cells (Figure 2D).

In the Triton-soluble fraction, PI3KC2β was constitutively associated with Grb2, and EGF stimulation promoted the interaction of the enzyme with the activated EGFR, Shc, Eps8, and Sos-1 (Figures 1A and 2D). In contrast, in the Triton-insoluble fraction, PI3KC2β was constitutively associated with the activated EGFR, Grb2, Eps8, and Sos-1 (Figures 1B, 2, A and B, and 3A). The constitutive association of the complex in the Triton-insoluble fraction was possibly caused by basal activation of the EGFR, either by autocrine TGF-α production, or overexpression of the receptor in A-431 cells (Van de Vijver *et al.*, 1991; Jo *et al.*, 2000).

To identify the domains of PI3KC2β and Eps8 involved in the formation of the complex in A-431 cells, we used pull-down assays with immobilized recombinant GST-domains. The N-terminal region of PI3KC2β interacted with Eps8 in A-431 lysates, independently of EGF stimulation, but no interaction was observed between the PI3KC2β C2 domain and Eps8 (Figure 2E). This data correlated with the observation that this region of PI3KC2β interacts with Shc and Grb2 (Figure 1C). The N-terminal region of Eps8 (residues 1–535) and its SH3 domain both interacted with PI3KC2β in lysates from unstimulated A-431-C2β WT cells (Figure 2F). However, the Eps8 PTB domain failed to bind to PI3KC2β in a comparable manner (Figure 2F). Thus, multiple surfaces of interaction are likely to participate in the formation of an Eps8-PI3KC2β complex.

Assembly of the Grb2-PI3KC2β-Eps8-Abi1-Sos1 Multiprotein Complex

To establish whether the Shc/Grb2/PI3KC2β and the PI3KC2β/Eps8/Abi1/Sos1 complexes were mutually exclusive complexes or one macromolecular complex, we investigated whether Grb2 could coimmunoprecipitate with Eps8. Grb2 immunoprecipitates from the Triton-insoluble fraction of A-431-C2β WT cells contained PI3KC2β and Eps8 as well as Sos1 (Figure 3A). Interaction mapping of the Eps8-Abi1-Sos1 Rac GEF ternary complex has shown that Abi1 acts as a scaffold protein, which holds together Eps8 and Sos1 (Fan and Goff, 2000; Scita *et al.*, 2000). More specifically, the ternary complex is assembled through binding of the Abi1 and Eps8 SH3 domains to the proline rich motifs of Sos1 and Abi1, respectively.

Profile motif scanning of Abi1 and Eps8 with a peptide library–based searching algorithm (Yaffe *et al.*, 2001) indicated a putative proline-rich Grb2 binding site on Abi1 (NIADSPTPPPPPD). GST-Grb2 fusion protein pulldowns demonstrated that Abi1 and Eps8 predominantly associated with the N-terminal SH3 domain of Grb2 (Figure 3B). In addition, endogenous Abi1 coimmunoprecipitated with Grb2 (Figure 3C), consistent with the observed coimmunoprecipitation of Abi1 and Grb2 in an independent study (Fan and Goff, 2000). To determine the physiological relevance of this complex, we investigated whether endogenously expressed Grb2 associated with the Eps8/Abi1/Sos1 Rac GEF ternary complex. Consistent with earlier findings (Fan and Goff, 2000), we observed coimmunoprecipitation of Abi1 with endogenously expressed Grb2, Eps8, and Sos1, as well as PI3KC2β (Figure 3D). Moreover, assembly of the Grb2-PI3KC2β-Eps8-Abi1-Sos1 complex was observed in two independent A-431 clones expressing kinase-dead PI3KC2β (A-431-C2β DN-17 and DN-32) implying that PI3KC2β lipid kinase activity is not required for the assembly of this complex (unpublished data).

These findings suggest that Grb2, Eps8, Abi1, Sos1, and PI3KC2β can assemble into a single complex in A-431 cells upon EGF stimulation (Supplementary Figure 3). We favor a model whereby PI3KC2β is complexed with the Eps8-Abi1-Sos1 ternary complex through direct binding of the N- and C-terminal SH3 domains of Grb2 to Abi1 and PI3KC2β, respectively (Supplementary Figure 3). However, the possibility that additional interactions occur in this multiprotein complex cannot be ruled out. Analysis of PI3K kinase activity in the presence of calcium ions, which are inhibitory to class I PI3Ks but can be utilized by class II enzymes (Arcaro *et al.*, 1998), indicated associated class II PI3K enzymatic activity was in the Grb2, Shc, Eps8, and Abi1 immune-complexes (Figure 3E). EGF stimulation did not stimulate PI3KC2β activity in Grb2 immunoprecipitates (Figure 3E), which was consistent with the constitutive association between the two proteins (Figures 1G and 2D). In contrast, a marked increase in associated PI3KC2β kinase activity was observed in Shc, Eps8, and Abi1 immunoprecipitates after EGF stimulation, which probably reflects increased or stabi-

Figure 1 (cont). (G) The A-431-C2β WT cell line was induced with 1 nM EGF for the times indicated before immunoprecipitation with Shc and Grb2. Analysis of the respective immune-complexes indicates that Grb2 and the p46/p52Shc isoforms both associate with PI3KC2β. (H) A-431 cell lysates were immunoprecipitated with Actigel coupled phosphorylated and nonphosphorylated peptides representing the EGFR-1 SH2-binding peptides for Grb2 (pY1068/Y1068) and Shc (pY992/992). The amount of endogenous PI3KC2β pulled down was determined by immunoblotting.

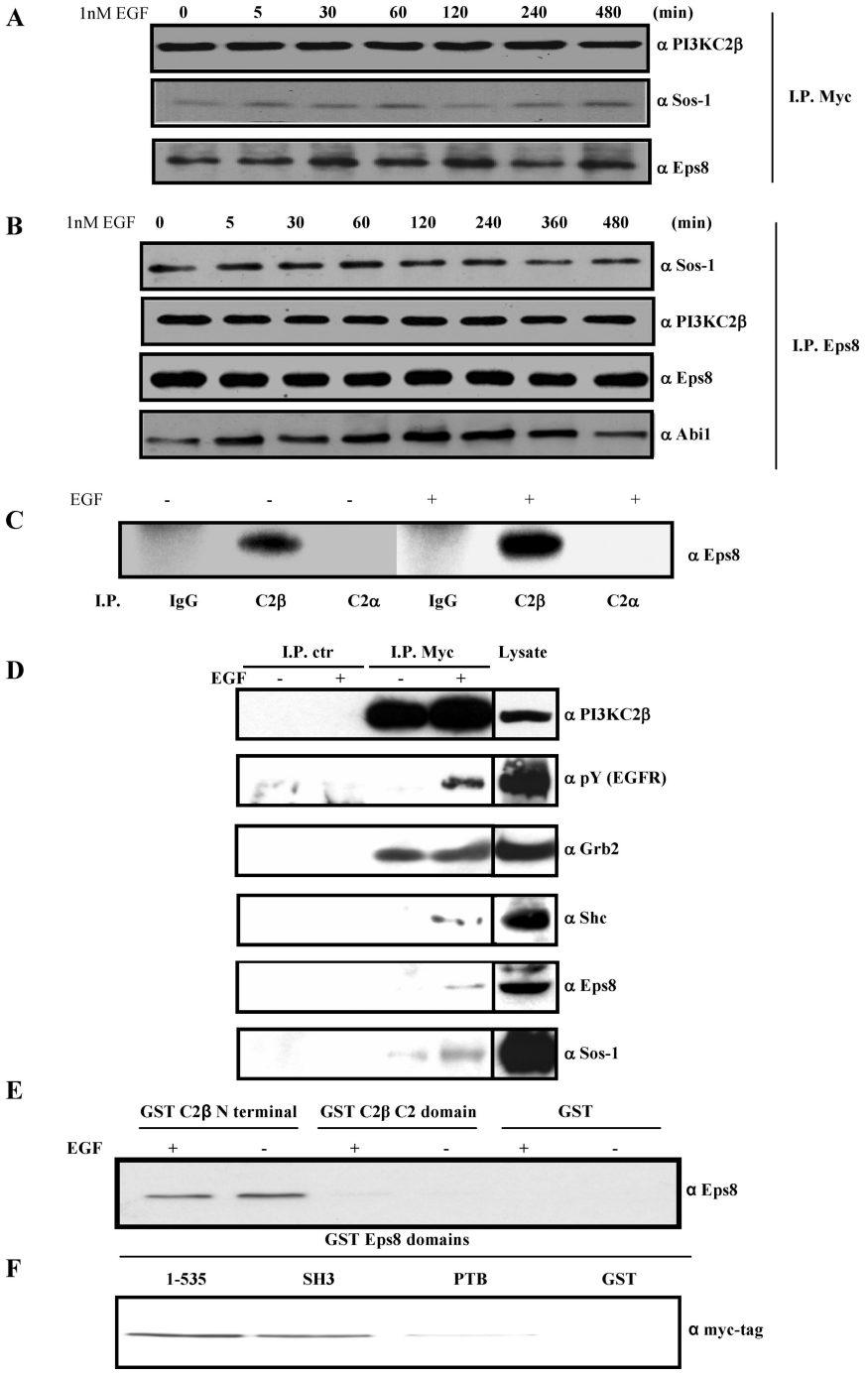

Figure 2. PI3KC2β associates with the Eps8-Abi1-Sos1 Rac GEF ternary complex. (A and B) A-431-C2β WT cells were stimulated with EGF for the indicated time points and then lysed. The Triton X-100–insoluble fractions were solubilized in RIPA buffer and then incubated with antibodies to PI3KC2β (A) or Eps8 (B). Immunoprecipitates were resolved by SDS-PAGE and then Western blots were probed with antibodies to Eps8 or Sos1 (A), or PI3KC2β, Eps8, Abi1, and Sos1. (C) Endogenous PI3KC2β and Eps8 associate in HEK293 cells. Triton X-100–soluble lysates from serum-starved (−) and EGF-induced (+) HEK293 cells were immunoprecipitated with antibodies to PI3KC2α, PI3KC2β, or control rabbit immunoglobulin (IgG). Immunoprecipitates were resolved by SDS-PAGE and Western blotted with antibodies to Eps8. (D) A-431-C2β WT cells were stimulated with EGF for 10 min. The Triton X-100–soluble fraction was immunoprecipitated with immobilized anti-Myc tag or control (mouse IgG) antibodies. Associated proteins were identified by immunoblotting with the indicated antibodies. Cell lysate was analyzed in parallel (20% of total lysate used in the immunoprecipitations). (E) Lysates from quiescent or EGF-stimulated A-431 cells were incubated with immobilized GST, or GST-domains corresponding to PI3KC2β N-terminal region or C2 domain. The samples were analyzed by Western blot with anti-Eps8 antibodies. (F) Lysates from A-431-C2β WT cells were incubated with immobilized GST, or GST-domains corresponding to Eps8 N-terminal region (residues 1–535) SH3, or PTB domain. The samples were analyzed by Western blot with anti-Myc tag antibodies.

lized association of PI3KC2β with the respective proteins (Figures 1 and 2).

PI3KC2β Regulates Rac Activity, Epithelial Adherens Junctions, and Membrane Ruffling

Targeted disruption of Eps8 results in a reduction in platelet-derived growth factor (PDGF)-induced membrane ruffling, Rac activation, and consequently JNK activation in fibroblasts (Scita *et al.*, 1999). Eps8 interacts with Abi1 and Sos to regulate the Rac GEF activity of Sos (Scita *et al.*, 2001; Innocenti *et al.*, 2002, 2003). To establish whether PI3KC2β affected Rac activity, A-431 cells were transfected with either Myc-tagged wild-type PI3KC2β (A-431-C2β WT) or a kinase-dead PI3KC2β that was rendered catalytically inactive by mutation of the highly conserved aspartate (***D***FG) to an alanine residue in the activation domain (D1213A, DN). Lipid immune-complex kinase assays of the respective Myc-tagged PI3KC2β proteins demonstrated that PI3KC2β D1213A (DN) was indeed catalytic inactive (Supplementary Figure 1A). The Cdc42/Rac interactive binding region (CRIB) domain of PAK1 that binds specifically to active GTP-bound Rac (Sander *et al.*, 1998) was used to assess Rac1 activity in the A-431–derived cell lines. In comparison to parental A-431 cells, basal and EGF-stimulated Rac1 activities were significantly

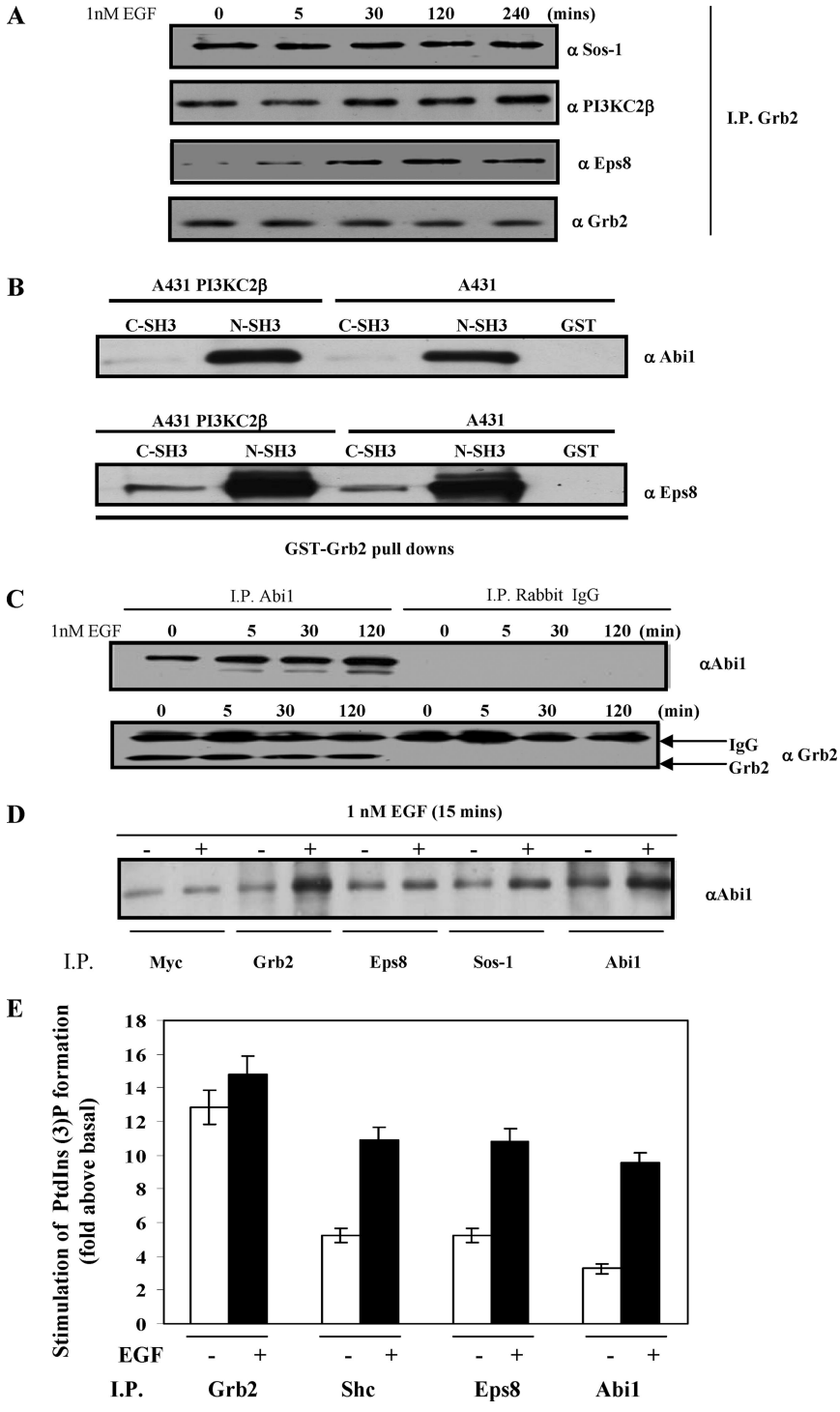

Figure 3. Assembly of the Grb2-PI3KC2β-Eps8-Abi1-Sos multiprotein complex. (A) Grb2 was immunoprecipitated from Triton X-100–insoluble A-431-C2β WT cell lysates and probed with the antibodies to Sos1, PI3KC2β, Eps8, and Grb2. (B) Abi1 interacts with Grb2. Lysates from A-431 and A-431-C2β WT cell line were immunoprecipitated with either the N- or C-terminal SH3 Gst-Grb2 fusion proteins. Precipitated proteins from the respective lysates were immunoblotted with Abi1 and Eps8. (C) Abi1 and control rabbit Immune-globulin complexes from Triton X-100–insoluble lysates of A-431 cells were Western-blotted with anti-Abi1 and anti-Grb2 antibodies. (D) A-431-C2β WT cells were serum-starved for 24 h (−) and stimulated with EGF for 5 min (+). Cell lysates were immunoprecipitated with antibodies to Myc, Grb2, Eps8, Abi1, or Sos1 then Western blotted with antibodies to Abi1. (E) Immune-complex class II PI3K lipid kinase activity was evaluated in the presence of calcium ions as previously described (Arcaro *et al.*, 1998). The results represent the mean of two independent experiments.

increased in A-431-C2β WT cells (Figure 4A). In contrast, Rac1 activity was notably decreased in the A-431-C2β DN cells (Figure 4A) implying that PI3KC2β lipid kinase activity regulates Rac1. Consistent with this observation, EGF-stimulated JNK1/2 activity and c-Jun phosphorylation were upregulated in A-431-C2β WT cells compared with wild-type A-431 cells (Figures 4, B and C). Conversely, JNK1/2 activity and c-Jun phosphorylation were decreased in the A-431-C2β DN cells (Figure 4, B and C). Basal and EGF-stimulated activation of Erk1/2 were attenuated in either A-431-C2β WT or DN cells, as compared with wild-type A-431 cells (Figure 4D). In contrast, activation of Akt1 was comparable between A-431 and A-431-C2β WT cell lines, as assessed by EGF-stimulated induction of Ser473 phosphorylation (Figure 4E). Thus PI3KC2β catalytic activity selectively regulates Rac1 activation in response to EGF in A-431 cells, which impacts on JNK1/2 activity and c-Jun phosphorylation. In contrast, PI3KC2β overexpression attenuates Erk1/2 activation independently of its lipid kinase activity in A-431 cells.

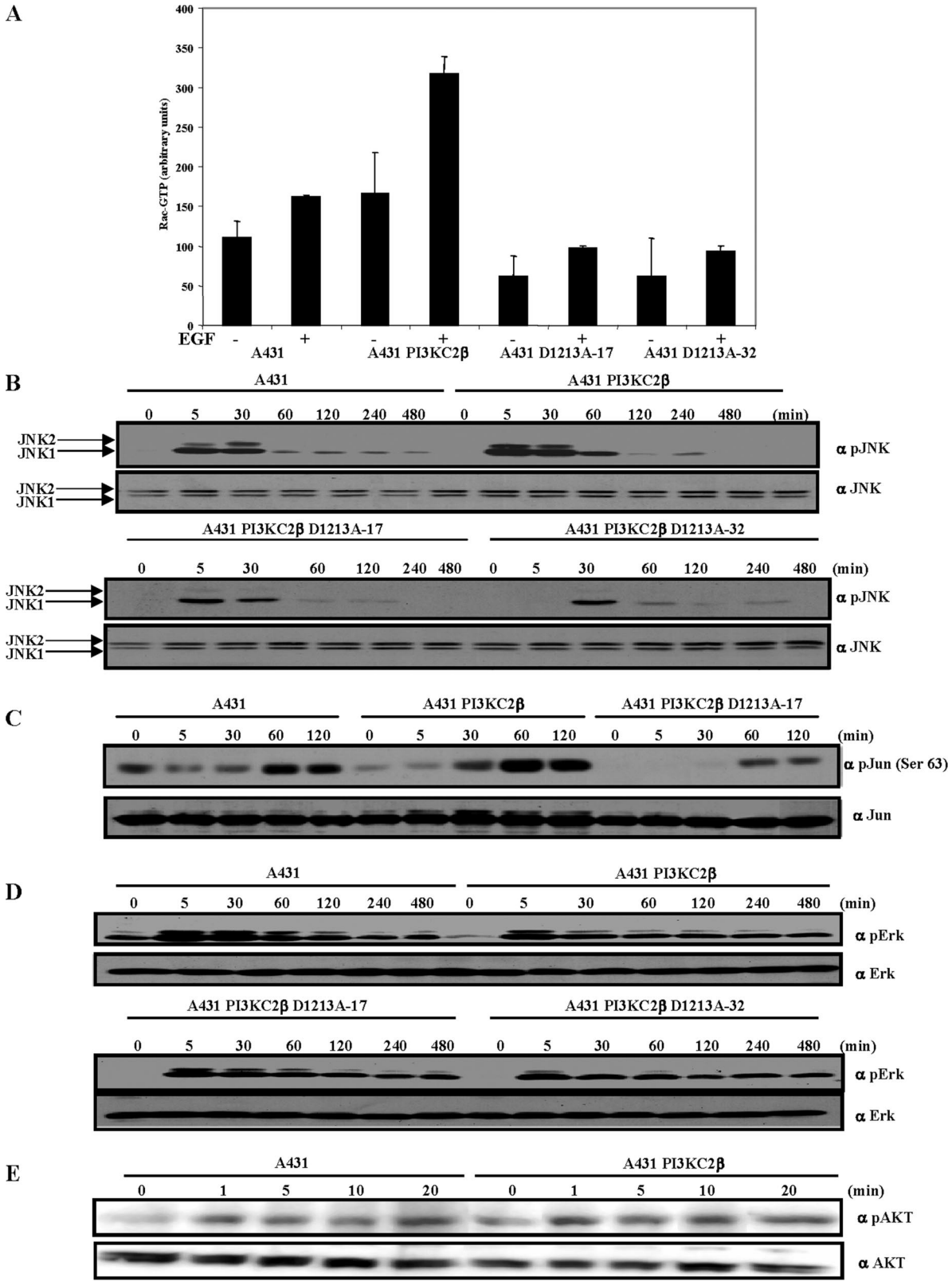

Figure 4. PI3KC2β regulates Rac and JNK activity. (A) PI3KC2β up-regulates Rac activity. Parental A-431 cells, and A-431 expressing wild-type PI3KC2β and kinase-dead PI3KC2β (D1213A-17, D1213A-32) were serum-starved for 24 h and stimulated with 1 nM EGF (+) for 5 min. The cell lysates were equalized for protein content before immunoprecipitation with GST-PAK CRIB. Immunoprecipitated and total Rac was detected by immunoblotting with a Rac mAb. The blots were quantified by densitometry. Data are mean with SD from four experiments. (B–E) A-431, A-431 cells expressing wild-type or kinase-dead PI3KC2β (D1213A-17, D1213A-32) were made quiescent by culturing in serum-free medium for 24 h before stimulation with 1 nM (C–D) or 8 nM (E) EGF for the times indicated. The Triton-soluble

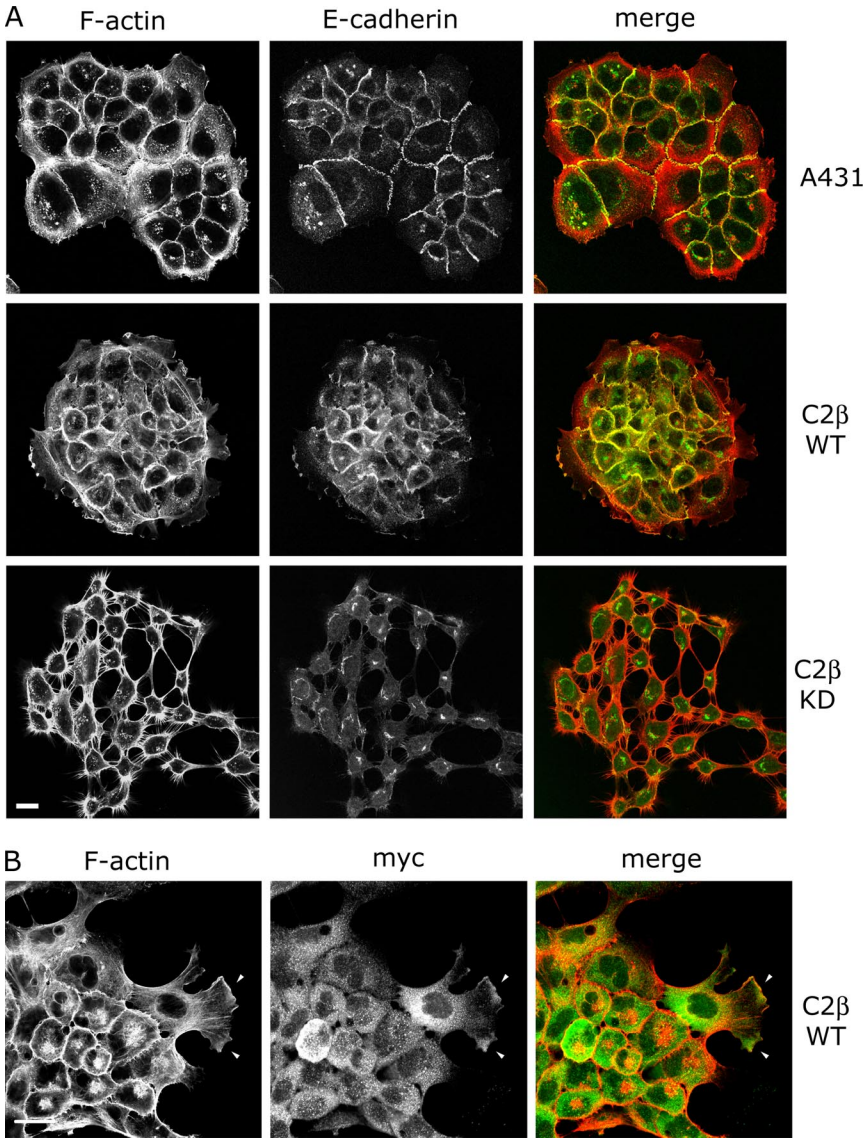

Figure 5. Effects of PI3KC2β on F-actin and adherens junctions. (A) Growing parental A-431 cells, A-431-C2β WT cells (WT), or A-431-C2β DN-32 (KD) cells were fixed and incubated with antibodies to E-cadherin followed by FITC-labeled anti-mouse antibodies and TRITC-labeled phalloidin to localize F-actin. (B) Growing PI3KC2β Myc-6 cells (WT) were fixed and stained with antibodies to the Myc epitope to localize PI3KC2β followed by FITC-labeled anti-mouse antibodies and TRITC-labeled phalloidin to localize F-actin. Arrows indicate PI3KC2β localization in lamellipodia. Bars (A and B), 10 μm.

A striking phenotypic consequence of increased PI3KC2β expression was that the A-431-C2β WT cells formed more compact colonies compared with parental A-431 cells (Supplementary Figure 1B). This phenotypic change is unlikely to be due to clonal variation as it was observed in three independent clones. Conversely, two independent PI3KC2β D1213A-expressing lines (A-431-C2β DN-17 and DN-32) exhibited a reduction in cell–cell contacts (Supplementary Figure 1C and unpublished data).

Analysis of the actin cytoskeleton of A-431-C2β WT cells revealed that PI3KC2β expression induced an increase in F-actin and E-cadherin at cell–cell junctions (Figure 5A), which is in agreement with the observed effects of activated Rac in enhancing adherens junction formation in epithelial cells (Braga *et al.*, 1997; Takaishi *et al.*, 1997). Similar effects were observed in two additional PI3KC2β-expressing cell lines, PI3KC2β Myc-4 and Glu-15 (unpublished data). PI3KC2β showed a predominantly punctate distribution in the cytoplasm and also localized to cell protrusions and ruffling regions of the plasma membrane in cells at the edge of colonies (Figure 5B, arrows), similar to the reported localization of Eps8 and Abi1 (Scita *et al.*, 2001; Stradal *et al.*, 2001). The level of PI3KC2β expression varied within colonies, and in the highest expressing cells there was a clear increase in the level of polymerized actin at cell–cell junctions, in the perinuclear region and in lamellipodia-like extensions. (Figure 5, A and B). The perinuclear accumulation of F-actin may reflect a role for Rac in regulating actin assembly on the Golgi (Fucini *et al.*, 2002). In contrast, A-431-C2β DN cells did not form stable adherens junctions when subconfluent and showed an increase in the level of intracellular perinuclear E-cadherin (Figure 5A). F-actin staining

Figure 4 (cont). extracts were equalized for protein content, resolved on duplicate gels, and probed with the indicated antibodies. The extent of JNK, Jun, Erk, and Akt activation was assessed in the respective cell lines by immunoblotting with phospho-specific antibodies directed against the activated forms of the proteins. The amount of total protein was established by blotting the duplicate blots with antibodies against JNK, c-Jun, Erk, and Akt. The positions of the bands corresponding to JNK1 (p46) and JNK2 (p54) are indicated by arrows.

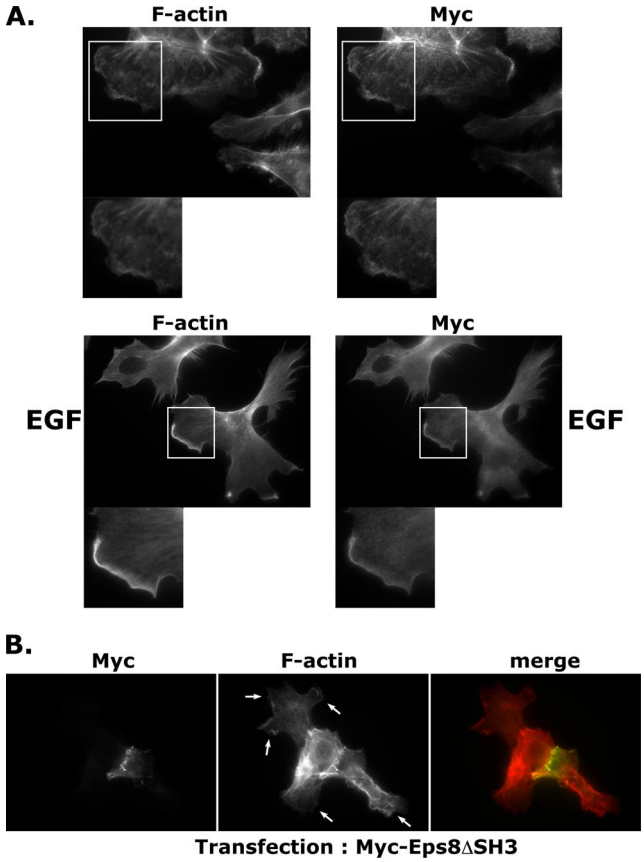

Figure 6. PI3KC2β is localized to lamellipodia in EGF-stimulated A-431 cells. (A) PI3KC2β-expressing cells were incubated for 24 h in a serum-free medium (top) or stimulated with 100 ng/ml EGF for 10 min (bottom). Cells were fixed and stained with phalloidin and anti-Myc antibody to visualize PI3KC2β. (B) A mutant of Eps8 unable to form a complex with Abi1, Eps8ΔSH3, impairs lamellipodia formation in A-431 PI3KC2β-expressing cells. PI3KC2β-expressing cells were transiently transfected with myc-Eps8ΔSH3. After 24 h, cells were fixed and stained with anti-Myc antibody and phalloidin. Lamellipodia, indicated by arrows, were inhibited in roughly 60% of Eps8ΔSH3-expressing cells.

of A-431-C2β DN cells revealed that cells often remained associated via fine F-actin–containing microspikes (Figure 5A). Filopodial extension has been implicated as one of the initial steps in adherens junction assembly (Vasioukhin *et al.*, 2000), where juxtaposed cells initially attach via filopodia to promote actin polymerization and clustering of E-cadherin at the site of cell–cell contact. It is therefore possible that A-431-C2β DN cells retain the ability to extend filopodia, but are unable to activate Rac in order to stabilize cell–cell adhesion.

Because the biochemical analysis had revealed a translocation of PI3KC2β to the Triton-insoluble cytoskeletal fraction upon EGF stimulation (Figure 1B), we sought to further investigate changes in PI3KC2β localization in response to A-431 cell stimulation. Serum-starved A-431-C2β WT cells were stimulated with EGF and localization of F-actin and Myc-tagged PI3KC2β assessed by immunofluorescence. Co-localization of PI3KC2β with F-actin in lamellipodia was observed in EGF-stimulated A-431-C2β WT cells (Figure 6A, bottom panel). An enrichment of PI3KC2β was observed at the leading edge of EGF-stimulated A-431-C2β WT cells, compared with serum-starved cells (Figure 6A, top panel).

Our data had revealed an association of PI3KC2β with the Eps8-Abi1-Sos-1 complex (Figures 1 and 2), implicated in the regulation of Rac activity. To confirm the role of this macromolecular complex in the regulation of Rac-dependent cytoskeletal rearrangements, A-431-C2β WT cells were transfected with an Eps8 mutant carrying a small deletion of four amino acids (538–542) in the SH3 domain (Eps8ΔSH3, Myc tag). This mutant Eps8 was previously reported to be unable to form a complex with Abi1 (Scita *et al.*, 1999). Staining of transfected A-431-C2β WT cells with anti-Myc tag antibodies and phalloidin revealed a strong (60%) decrease of lamellipodia formation in Eps8ΔSH3-expressing cells (Figure 6B). Thus, perturbing the Eps8-Abi1-Sos-1 complex inhibits Rac-dependent cytoskeletal rearrangements in A-431-C2β WT cells.

We next further studied membrane ruffling in A-431 and PI3KC2β transfectants and its dependence on Rac function. Lamellipodia, were detected in at least 70% of EGF-treated A-431 cells, but not (0%) in serum-starved cells (Figure 7A). More than 60% of the PI3KC2β-expressing cells displayed lamellipodia-like extensions in the absence of EGF stimulation. (Figure 7B; see also Supplementary Videos 1 and 2). EGF-stimulated lamellipodia formation was inhibited by transfection of RacN17 into A-431 cells (Figure 7C). Moreover, lamellipodia extension by PI3KC2β-expressing cells in serum-free medium was also inhibited by RacN17 transfection (Figure 7D). Thus PI3KC2β enhances Rac-dependent lamellipodium formation.

PI3KC2β-transfected Cells Display a Rac and PI3K-dependent Increase in Cell Migration

Because of the reported role of Rac in regulating cell motility (Pankov *et al.*, 2005; Yamauchi *et al.*, 2005), we also wanted to investigate the effects of the PI3KC2β-mediated increase in Rac1 activation on A-431 cell migration. To this effect, A-431 and A-431-C2β WT cells were plated at 25% confluence, and their migration pattern was followed by time-lapse microscopy over a period of 18 h. Cell tracks were then analyzed using Mathematica notebooks to determine the Gaussian distribution of migration speeds (Figure 8, A and C) as well as the medium radius from start covered by cells in each condition (Figure 8B). Figure 8, A and C show that PI3KC2β-tansfected cells migrated consistently faster than their parental A-431 counterparts either in the presence or absence of EGF, a growth factor reported to increase A-431 cell motility (Sparatore *et al.*, 2005). We also noticed that the RNAi-mediated down-regulation of Rac1 (Supplementary Figure 2), had opposite effects on A-431-C2β WT and A-431 cell migration. Although the Rac siRNA increased A-431 migration speed, it counteracted the class II PI3K-mediated increase in A-431 cell motility, reverting them to the parental phenotype (Figure 8C). However, these changes in migration speed did not translate into an increase of the area covered by the migrating cells as demonstrated by horizon calculation (Figure 8B). Horizon calculation is a representation of the mean radius of the area covered by the migrating cell from its starting point. Increase in the value of the radius covered represents an increased persistence in cell movement as opposed to randomness. Indeed, only EGF stimulation allowed A-431 and A-431-C2β WT cells to migrate further from their starting point (Figure 8B). This is also consistent with the observation that A-431-C2β WT cells display a fast rate of randomly forming membrane protrusion with respect to A-431 cells (Figure 7, Supplemen-

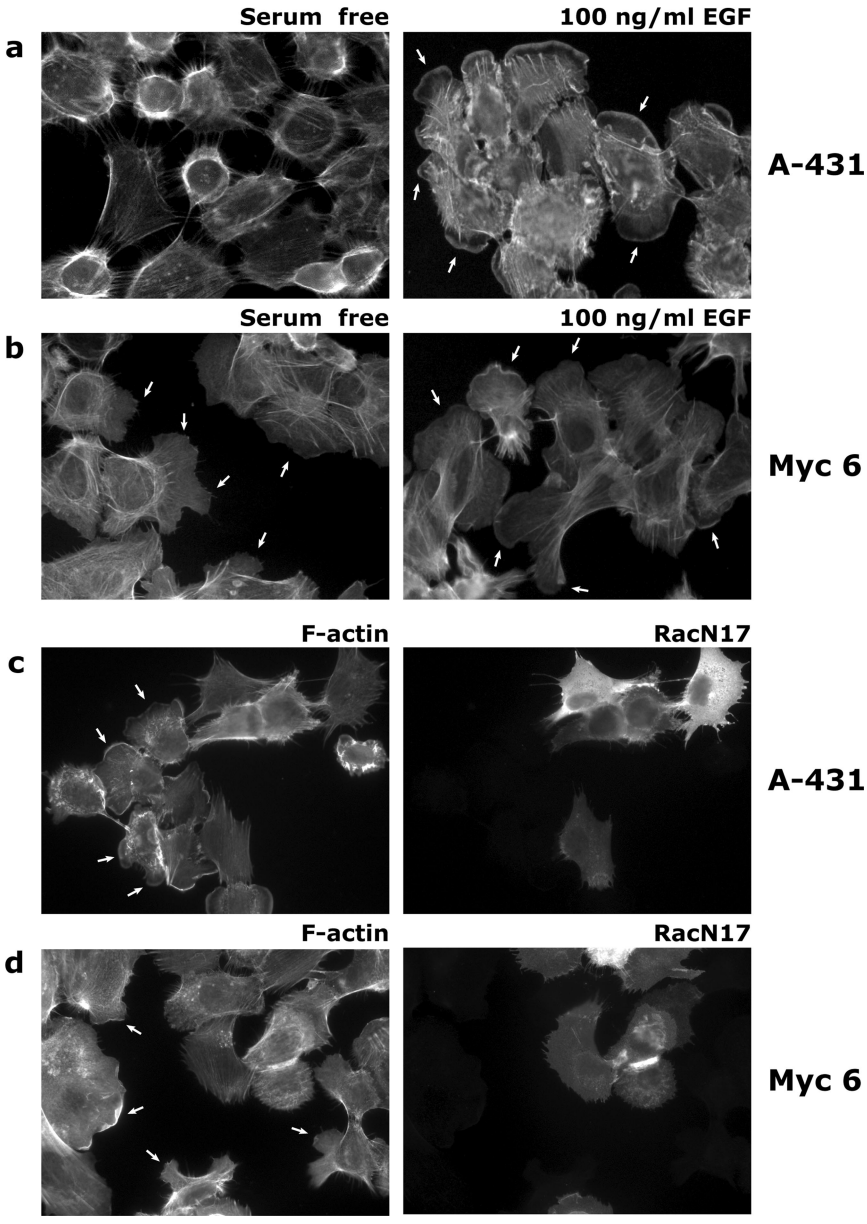

Figure 7. PI3KC2β expression induces lamellipodia constitutively in a Rac-dependent manner. Serum-deprived A-431 control (A) or A-431 PI3KC2β-expressing cells (Myc 6; B) were stimulated with 100 ng/ml EGF for 10 min (right panels) or left untreated (left panels), fixed, and stained with phalloidin to detect F-actin. (C) A-431 control cells were transiently transfected with HA-RacN17, serum-starved, and stimulated with 100 ng/ml EGF. Cells were fixed and stained with anti-HA antibodies and phalloidin. Lamellipodia, indicated by arrows, are inhibited in all RacN17-expressing cells. (D) PI3KC2β-expressing A-431 cells (Myc 6) were transiently transfected with HA-RacN17. Cells were then fixed and stained as in C. Lamellipodia extensions, indicated by arrows, were inhibited in 100% of RacN17-expressing cells.

tary Videos 1 and 2). These data suggest that although PI3KC2β overexpression provides A-431 cells with increased motility speeds, it does not allow for migratory directional persistence. In support of this notion, the migration speed of A-431 cells expressing dominant negative PI3KC2β was significantly decreased, compared with wild-type A-431 cells (Figure 8D). Moreover, the area covered by migrating A-431-C2β DN cells was reduced, compared with control A-431 cells (Figure 8E). Thus, PI3KC2β catalytic activity is also required for migratory directional persistence.

PI3KC2β Expression Increases Cell Proliferation and Renders A-431 Cells Resistant to Anoikis

We next investigated whether the differences in activation of early signaling events observed between A-431 and PI3KC2β-transfected cells (Figure 4) correlated with changes in proliferation and survival of the cells. Proliferation of A-431-C2β WT cells was elevated by ~1.75-fold, as compared with A-431 cells (Figure 9A). This difference was observed both in medium containing low (1%) or high (10%) serum (unpublished data). To investigate whether the increased proliferation of A-431-C2β WT was dependent on the function of JNK or Akt, pharmacological inhibitors of both kinases were tested on both A-431 and A-431-C2β WT cells. The Akt inhibitor (1L-6-hydroxymethyl-chiro-inositol 2-(R)-2-*O*-methyl-3-*O*-octadecylcarbonate) failed to reduce the difference in proliferation between both cell lines at concentrations up to 20 μM (unpublished data). At these concentrations, however, it completely inhibited growth of human neuroblastoma cell lines (unpublished data). A cell-permeable peptide inhibitor of JNK translocation (reported IC_{50} = 1 μM for JNK inhibition) also did not reduce the proliferation of either cell line, although at high concentrations (>25 μM) it reduced proliferation of A-431-C2β WT cells (Figure 9B).

Anoikis is a form of cell death induced by cell detachment from the underlying substratum. Resistance to anoikis is re-

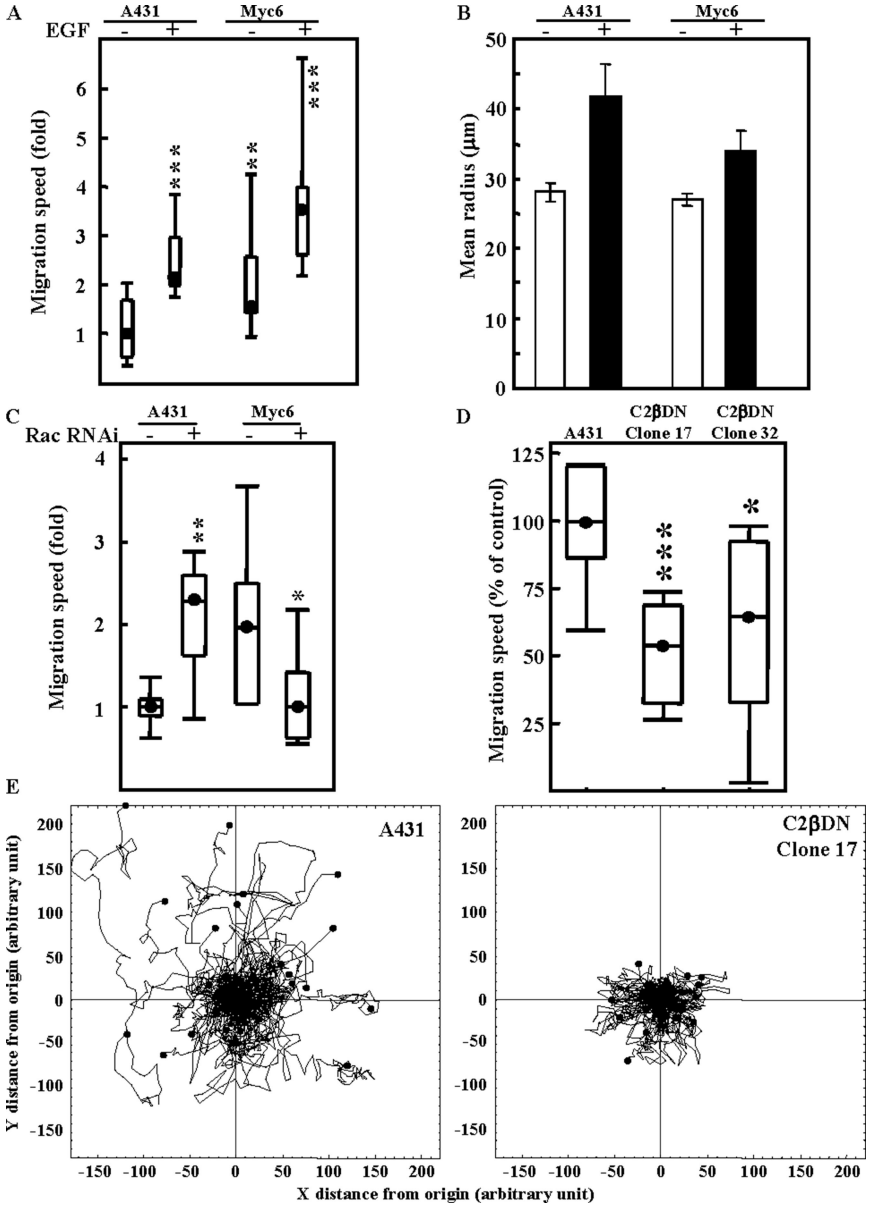

Figure 8. Rac1 RNAi differentially affect A-431 and A-431-C2β WT cell migration. (A and B) A-431 and A-431-C2β WT cells (Myc 6) cells were treated with or without EGF. (C) A-431 and A-431-C2β WT cells were transfected with Rac1 RNAi or scrambled control (−) and left for 48 h in culture to achieve target down-regulation. Cell migration tracks were monitored by live microscopy for 18 h, and migration speed (A and C) or horizon radius (B) was determined using Mathematica. These results are representative of a minimum of three independent experiments. Each condition was performed in quadruplicate using 15 cells per replicate. (D and E) Cell migration tracks of A-431 cells, or A-431 expressing kinase-dead PI3KC2β (C2β DN-17, C2β DN-32) were monitored by live microscopy for 18 h, and migration speed (D), or track paths (E) were determined using Mathematica. Results are representative of a minimum of three independent experiments. Each condition was performed in quadruplicate using 15 cells per replicate. (Significant difference as compared with control A-431 (A and D) or between Rac1 RNAi and scrambled control (C); Student's *t* test: *$p < 0.05$; **$p < 0.01$; ***$p < 0.001$).

quired for tumor cells to establish remote metastasis (Liotta and Kohn, 2004). Therefore, experiments were conducted to investigate whether PI3KC2β expression modified the survival of A-431 cells. A-431 and PI3KC2β-transfected cells were allowed to keep in suspension by plating on ultralow attachment dishes. After 12-h incubation at 37°C, the cells were fixed and stained by propidium iodide for flow cytometry analysis of DNA content. The proportion of dead cells was measured by detecting cells in the sub-G1 fraction of the DNA profile. Figure 9C shows that the proportion of cells in sub-G1 was twice as high in A-431 as in A-431-C2β WT cells (≈30% vs. ≈15%). This difference maintained even at 24-h after detachment (Figure 9D), showing that PI3KC2β expression provides A-431 cells with a long-lasting protection from cell death. In both cell lines, addition of EGF inhibited the induction of anoikis (Figure 9, C and D), as previously described (Jost *et al.*, 2001; Reginato *et al.*, 2003). This decrease in the proportion of cells in sub-G1 correlated with an inhibition of phosphatidylserine exposure in PI3KC2β-transfected cells as demonstrated after Annexin V staining (Figure 9E). Taken together these results demonstrate that expression of class II PI3K desensitizes A-431 cells to the induction of anoikis.

Rac1 and E-Cadherin Do Not Mediate the Resistance of PI3KC2β-transfected Cells to Anoikis

Our previous data had revealed that PI3KC2β-transfected cells display an increase in Rac1 activation and E-cadherin levels (Figures 4 and 5). As these two proteins have been linked to cell survival in other cell systems (Murga *et al.*, 2002; Ferreira *et al.*, 2005), we investigated the possibility that they might participate to Myc6 cells resistance to anoikis. However, down-regulation of Rac1 using oligonucleotide RNAi (Supplementary Figure 2C) had no effect on either A-431-C2β WT or A-431 cell survival after cell detachment (Supplementary Figure 2A). Similarly, E-cadherin inhibition using neutralizing antibodies, although decreasing cell–cell contacts in A-431-C2β WT cells back to the extent

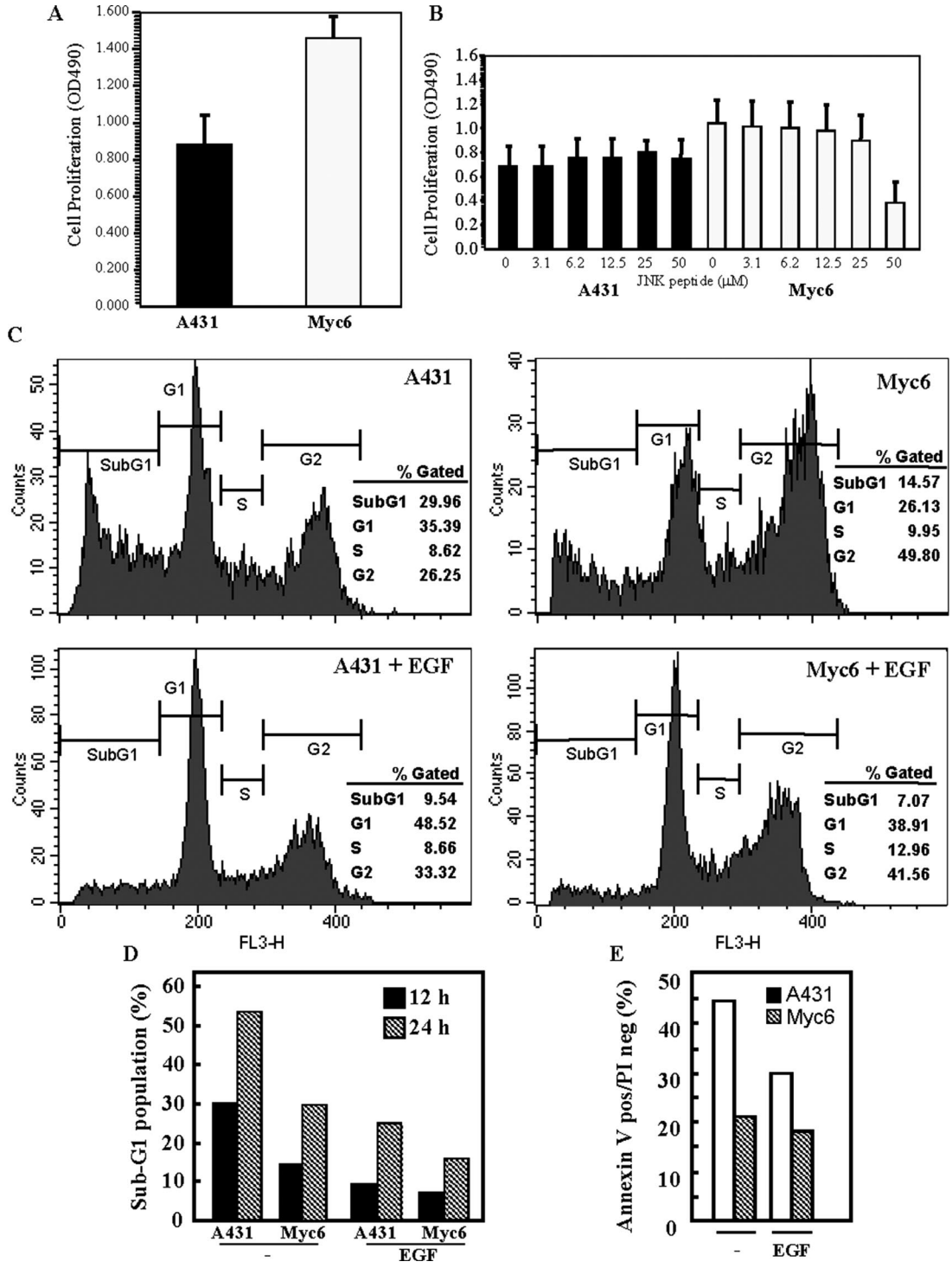

Figure 9. PI3KC2β-transfected A-431 cells display enhanced proliferation and are resistant to anoikis. (A and B) A-431 and A-431-C2β WT (Myc 6) cells were incubated for 72 h in medium containing 1% serum in the absence (A) or presence (B) of increasing concentrations of a cell-permeable JNK inhibitor peptide. Cell proliferation was assessed using a MTS assay. Data are mean with SD from eight repetitions. (C–E) A-431 and A-431-C2β WT (Myc 6) cells were placed for 12 h (C–E) or 24 h (D) in anchorage-free conditions in the presence or absence of EGF. Cells were then stained using propidium iodide alone (C and D) or in conjunction with annexin V (E) and the proportion of cells in SubG1 (C and D) or positive for annexin V only (E) determined by flow cytometry.

observed in A-431 cells (Supplementary Figure 2D), did not impair A-431-C2β WT cells' ability to resist anoikis (Supplementary Figure 2B). Therefore, neither Rac1 nor E-cadherin appear to contribute to the difference in sensitivity to anoikis that exist between A-431 and A-431-C2β WT cells.

Detachment-induced Changes in Early Signaling Molecules Activation and Sensitivity to Anoikis of A-431 and PI3KC2β-transfected Cells

We then hypothesized that differences in the activation of early signaling molecules might be involved in the inhibi-

tion of anoikis after expression of the class-II PI3K. Hence, we determined the phosphorylation status of Erk, Akt, p38, and JNK in A-431 and A-431-C2β WT cells both while attached and 6 h after detachment.

The phosphorylation of p38 appeared unmodified by cell detachment (Supplementary Figure 2E) and incubation of A-431 or A-431-C2β WT cells with the p38 inhibitor, SB202190, although increasing to the same extent the baseline cell death level for both cell lines, did not counteract the effects of class II expression on A-431 survival to anoikis. This suggest that p38 is not involved in the survival advantage of A-431-C2β WT cells.

Although phosphorylation of Erk was equal in attached A-431 and Myc6 cells and remained identical in A-431-C2β WT cells upon detachment, the amount of activated Erk decreased noticeably in A-431 cells after 6 h in anchorage-free incubation (Supplementary Figure 2E). However, inhibition of mitogen-activated Erk kinase (MEK) in A-431-C2β WT cells using PD098059 did not prevent the inhibition of cell death observed in these cells upon detachment (Supplementary Figure 2F). This would suggest that differences in the activation of the MEK/Erk pathway between A-431 and A-431-C2β WT cells are not responsible for their differences in survival.

The phosphorylation of Akt increased in both A-431 and Myc6 cells upon detachment (Supplementary Figure 2E). Although the extent of this increase was similar in the two cell lines, the effects of Akt phosphorylation might still be differentially regulated in A-431 and A-431-C2β WT cells by downstream effectors of Akt. However, Supplementary Figure 2G demonstrates that RNAi-mediated down-regulation of Akt1 and 2 (Supplementary Figure 2C), in isolation or jointly, while increasing the level of cell death in both cell lines, did not prevent the prosurvival advantage of class II PI3K overexpression in A-431-C2β WT cells (Supplementary Figure 2G). Also, the inhibition of the downstream effector of Akt, mTOR (the mammalian target of rapamycin) by rapamycin, did not abolish the survival differential between A-431 and A-431-C2β WT cells (Supplementary Figure 2G). This suggests that changes in Akt phosphorylation cannot account for the class II–mediated inhibition of anoikis.

In contrast to activated Akt levels, the basal phosphorylation of JNK decreased sharply following detachment, both in A-431 and A-431-C2β WT cells (unpublished data). In addition, we found that down-regulation of the JNK upstream kinase, MKK7, by RNAi (Supplementary Figure 2C), while greatly increasing the death toll upon detachment of A-431 cells, had no similar effect on A-431-C2β WT cells survival (Supplementary Figure 2H).

DISCUSSION

The search for potential regulators or effectors of PI3KC2β signaling has identified Abi1, Eps8, and Sos as novel interaction partners of PI3KC2β. Our results show that PI3KC2β forms a complex with Eps8-Abi1-Sos1 upon EGF stimulation and that it regulates Rac activity. Class II PI3Ks preferentially generate PI(3)P and PI(3,4)P_2 in vitro (Arcaro *et al.*, 1998, 2000), but will generate PI(3,4,5)P_3 under certain conditions (Gaidarov *et al.*, 2001), and thus have the potential to generate the same spectrum of 3′-phosphoinositides as class I PI3Ks. We propose that one way through which PI3KC2β can activate Rac by producing phosphoinositides that activate Sos-1 Rac GEF activity in the PI3KC2β-Eps8-Abi1-Sos1 complex. Rac then controls membrane ruffling, cell motility, and cadherin-mediated cell–cell adhesion. Our data suggest that the major determinant in mediating an EGFR-PI3KC2β-Grb2-Eps8 complex is Grb2. Within this macromolecular unit, however, multiple surfaces of interaction are likely to stabilize the entire signaling unit. The PI3KC2β-Grb2-Abi1-Eps8-Sos1 complex could interact with the activated EGFR-1 either directly (pY1068) or indirectly (pY992) through complex formation with Shc. Interestingly, an interaction between the tyrosine phosphorylated p66Shc isoform with PI3KC2β was found specifically in the Triton-insoluble cytoskeletal fraction of EGF-stimulated A-431 cells. This observation may reflect a selective role for PI3KC2β and p66Shc in transducing signals controlling cytoskeletal rearrangements, because a recent report has shown that this Shc isoform plays a role Sos-mediated activation of Rac1 (Khanday *et al.*, 2006). EGFR-1 regulates this macro-molecular complex by stimulating PI3KC2β lipid kinase activity in the complex. Interestingly, a Shc-Grb2-Gab ternary complex has been shown to recruit class I PI3Ks to activated EGFR-1 (Rodrigues *et al.*, 2000), implying that there might be two distinct Shc-Grb2-PI3K class I and II complexes downstream of EGFR-1.

As A-431 cells produce and are constitutively activated by TGF-α acting on the EGFR-1 (Van de Vijver *et al.*, 1991; Jo *et al.*, 2000), it is likely that this induces sufficient PI3KC2β activation in PI3KC2β-overexpressing cells to transduce signals to Rac, without addition of EGF. Indeed, PI3KC2β transfection constitutively stimulated membrane ruffling and cell motility, and both responses were impaired by dominant negative Rac or RNAi. EGF can promote motility and invasion of A-431 cells (Malliri *et al.*, 1998), but is likely that other signals in addition to Rac activation are required for this response, as is the case in HGF-stimulated MDCK cells (Potempa and Ridley, 1998; Sander *et al.*, 1998). Indeed, down-regulation of Rac by RNAi had opposite effects on A-431 and A-431-C2β WT cells, enhancing the migration speed of the parental cells, while inhibiting the response of the transfectants. A possible model is that in A-431 cells Rac1 predominantly controls cell–cell contacts and thus functions as a negative regulator of cell motility. Interestingly, down-regulation of the Rac exchange factor Tiam1 was shown to induce disassembly of cadherin-based adhesions, resulting in enhanced migration of MDCK cells (Malliri *et al.*, 2004). In contrast, in A-431-C2β WT cells, where Rac1 is constitutively activated, it may function predominantly as a regulator of cell motility and membrane ruffling.

PI3K has been implicated in the regulation of E-cadherin–mediated adherens junction assembly in a number of independent studies (Nakagawa *et al.*, 2001; Kovacs *et al.*, 2002). However, these studies have used the generic PI3K inhibitors, wortmannin and LY294002, which do not discriminate between class I and class II PI3K-regulated events. Gene targeting studies have recently revealed a specific role for class I_A PI3K isoforms in cytoskeletal rearrangements, such as membrane ruffling stimulated by PDGF (Brachmann *et al.*, 2005). The relative contribution of class II or class I PI3Ks to Rac activation is thus likely to depend on the receptor utilized as well as the cellular context. Previous work has shown that the EGF receptor couples to class I_A PI3K signaling only in a cell type–specific manner (Arcaro *et al.*, 2000). Sos-1 can contribute to Rac activation both directly, through its Rac GEF domain and indirectly through activation of Ras by its Ras GEF domain and subsequent PI3K activation (Rodriguez-Viciana *et al.*, 1997). We have previously shown that in contrast to class I PI3Ks, PI3KC2β is not activated by Ras (Arcaro *et al.*, 1998). Therefore, although class I PI3Ks mediate Ras-dependent activation of Rac, PI3KC2β is likely to couple growth factor receptor signals to the Rac machinery in a Ras-independent manner. Although more work will be required to define the exact interplay of

the respective components, it is feasible that the divergent influence of Ras regulation of classes I and II PI3Ks upstream of Rac will also influence the cellular outcome. In conclusion, our results identify novel effectors of PI3KC2β cellular function and demonstrate for the first time a role for a class II PI3K in cytoskeletal activation by defining a molecular link between the EGFR-1, PI3KC2β, and Rac. A recent report has shown that PI3KC2β controls cell migration in response to lysophosphatidic acid (LPA) in human cancer cells such as HeLa cells (Maffucci *et al.*, 2005). It is at present unclear whether the same molecular mechanisms are involved in the ability of PI3KC2β to transduce signals from serpentine (LPA) or receptor tyrosine kinases (EGFR), although LPA is a known activator of Rac (Moolenaar *et al.*, 2004).

In contrast to its role in the regulation of cell motility and membrane ruffling, Rac1 appeared to play no role in PI3KC2β-induced protection of A431 from anoikis. The anti-apoptotic effect of PI3KC2β overexpression was also independent of Akt signaling, mTOR, and E-cadherin–mediated cell–cell contact. The observation that PI3KC2β-transfected cells display enhanced growth may thus be in part a result of this difference in survival. In agreement with the anoikis data, pharmacological inhibitors of JNK or Akt failed to affect the enhanced growth response observed in PI3KC2β-overexpressing A-431 cells. Pharmacological inhibition of MEK also failed to alter the response, but PI3KC2β-transfected A-431 cells displayed a more sustained activation of Erk1/2 than A-431 cells upon detachment. Thus, one cannot exclude the possibility that the differences in Erk activity between the two cell lines occur via a MEK-independent pathway (for example, protein kinase C [PKC] isoforms, phophatases; Grammer and Blenis, 1997; Bapat *et al.*, 2001; Kinkl *et al.*, 2001; Tajima *et al.*, 2005). EGF-stimulated activation of JNK was enhanced in PI3KC2β-transfected cells, correlating with the increase in Rac1 activation in these cells. Moreover, our data show that down-regulation of the JNK upstream kinase, MKK7 by RNAi, while greatly increasing detachment-induced apoptosis of A-431 cells, had no similar effect on A-431-C2β WT cells' survival. In line with the reported role of the JNK pathway in the survival of some cell systems (Wang *et al.*, 1999; Gururajan *et al.*, 2005), these data suggest that inhibition of JNK activity is toxic to A-431 cells and that class II overexpression might prevent this toxicity in A-431-C2β WT cells.

Although the present study was restricted to the A-431 cell line, we have found evidence that PI3KC2β interacts with Eps8 and regulates Rac activity in other human cancer cell lines. In human small cell lung cancer (SCLC) cell lines, which overexpress PI3KC2β, compared with normal lung epithelial cells (Arcaro *et al.*, 2002), an interaction between Eps8 and the class II PI3K was observed. SCLC cell lines expressing high levels of endogenous PI3KC2β had increased Rac activity and displayed enhanced JNK activation, compared with cell lines with low levels of PI3KC2β expression. Moreover, expression of kinase dead PI3KC2β in SCLC cells inhibited Rac and JNK activation (unpublished observations). Thus, the interaction of PI3KC2β with Eps8 involved in Rac activation may be of significance in various human cancer cells.

Together, the present report provides novel insights into the functions of class II PI3Ks in the context of human cancer. Human tumor cells have been reported to overexpress class II PI3K isoforms, such as PI3KC2β (Arcaro *et al.*, 2002). The ability of PI3KC2β to enhance migration and protect cells from anoikis may provide a crucial contribution to the malignant phenotype of various human cancers.

ACKNOWLEDGMENTS

We are grateful to Ritu Garg and Richard Foxon for technical assistance. We thank Dr. Paolo Di Fiore (European Institute of Oncology, Milan) for reagents and stimulating discussions during the preparation of the manuscript and John Collard (Netherlands Cancer Institute) for the pGEX-2T GST-PAK-CRIB expression vector. The Ludwig Institute of Cancer Research supported this research. Work in the laboratory of A.A. was supported by the Swiss National Science Foundation (Grant 3100A0–105321). Work in the laboratory of GS was supported by grants from the Human Science Frontier Program (Grant RGP0072/2003-C), Associazione Italiana Ricerca sul Cancro and the European Community (VI Framework). C.F. was supported by a graduate scholarship from the Boehringer-Ingelheim Foundation.

REFERENCES

Arcaro, A., Khanzada, U. K., Vanhaesebroeck, B., Tetley, T. D., Waterfield, M. D., and Seckl, M. J. (2002). Two distinct phosphoinositide 3-kinases mediate polypeptide growth factor-stimulated PKB activation. EMBO J. *21*, 5097–5108.

Arcaro, A., Volinia, S., Zvelebil, M. J., Stein, R., Watton, S. J., Layton, M. J., Gout, I., Ahmadi, K., Downward, J., and Waterfield, M. D. (1998). Human phosphoinositide 3-kinase C2beta, the role of calcium and the C2 domain in enzyme activity. J. Biol. Chem. *273*, 33082–33090.

Arcaro, A., Zvelebil, M. J., Wallasch, C., Ullrich, A., Waterfield, M. D., and Domin, J. (2000). Class II phosphoinositide 3-kinases are downstream targets of activated polypeptide growth factor receptors. Mol. Cell Biol. *20*, 3817–3830.

Bapat, S., Verkleij, A., and Post, J. A. (2001). Peroxynitrite activates mitogen-activated protein kinase (MAPK) via a MEK-independent pathway: a role for PKC. FEBS Lett. *499*, 21–26.

Brachmann, S. M., Yballe, C. M., Innocenti, M., Deane, J. A., Fruman, D. A., Thomas, S. M., and Cantley, L. C. (2005). Role of phosphoinositide 3-kinase regulatory isoforms in development and actin rearrangement. Mol. Cell Biol. *25*, 2593–2606.

Braga, V. M., Machesky, L. M., Hall, A., and Hotchin, N. A. (1997). The small GTPases Rho and Rac are required for the establishment of cadherin-dependent cell-cell contacts. J. Cell Biol. *137*, 1421–1431.

Fan, P., and Goff, S. P. (2000). Abl interactor 1 binds Sos and inhibits epidermal growth factor- and v-abl-induced activation of extracellular signal-regulated kinases. Mol. Cell Biol. *20*, 7591–7601.

Ferreira, P. *et al.* (2005). Loss of functional E-cadherin renders cells more resistant to the apoptotic agent taxol in vitro. Exp. Cell Res. *310*, 99–104.

Fucini, R. V., Chen, J. L., Sharma, C., Kessels, M. M., and Stamnes, M. (2002). Golgi vesicle proteins are linked to the assembly of an actin complex defined by mAbp1. Mol. Biol. Cell *2*, 621–631.

Gaidarov, I., Smith, M. E., Domin, J., and Keen, J. H. (2001). The class II phosphoinositide 3-kinase C2alpha is activated by clathrin and regulates clathrin-mediated membrane trafficking. Mol. Cell *7*, 443–449.

Grammer, T. C., and Blenis, J. (1997). Evidence for MEK-independent pathways regulating the prolonged activation of the ERK-MAP kinases. Oncogene *14*, 1635–1642.

Gururajan, M., Chui, R., Karuppannan, A. K., Ke, J., Jennings, C. D., and Bondada, S. (2005). c-Jun N-terminal kinase (JNK) is required for survival and proliferation of B-lymphoma cells. Blood *106*, 1382–1391.

Innocenti, M., Frittoli, E., Ponzanelli, I., Falck, J. R., Brachmann, S. M., Di Fiore, P. P., and Scita, G. (2003). Phosphoinositide 3-kinase activates Rac by entering in a complex with Eps8, Abi1, and Sos-1. J. Cell Biol. *160*, 17–23.

Innocenti, M., Tenca, P., Frittoli, E., Faretta, M., Tocchetti, A., Di Fiore, P. P., and Scita, G. (2002). Mechanisms through which Sos-1 coordinates the activation of Ras and Rac. J. Cell Biol. *156*, 125–136.

Jo, M., Stolz, D. B., Esplen, J. E., Dorko, K., Michalopoulos, G. K., and Strom, S. C. (2000). Cross-talk between epidermal growth factor receptor and c-Met signal pathways in transformed cells. J. Biol. Chem. *275*, 8806–8811.

Jost, M., Huggett, T. M., Kari, C., and Rodeck, U. (2001). Matrix-independent survival of human keratinocytes through an EGF receptor/MAPK-kinase-dependent pathway. Mol. Biol. Cell *12*, 1519–1527.

Katso, R., Okkenhaug, K., Ahmadi, K., White, S., Timms, J., and Waterfield, M. (2001). Cellular function of phosphoinositide 3-kinase: implications for development, immunity, homeostasis, and cancer. Annu. Rev. Cell Dev. Biol. *17*, 615–675.

Khanday, F. A. *et al.* (2006). Sos-mediated activation of rac1 by p66shc. J. Cell Biol. *172*, 817–822.

Kinkl, N., Sahel, J., and Hicks, D. (2001). Alternate FGF2-ERK1/2 signaling pathways in retinal photoreceptor and glial cells in vitro. J. Biol. Chem. *276*, 43871–43878.

Kovacs, E. M., Ali, R. G., McCormack, A. J., and Yap, A. S. (2002). E-cadherin homophilic ligation directly signals through Rac and phosphatidlyinositol 3-kinase to regulate adhesive contacts. J. Biol. Chem. *277*, 6708–6718.

Lanzetti, L., Rybin, V., Malabarba, M. G., Christoforidis, S., Scita, G., Zerial, M., and Di Fiore, P. P. (2000). The Eps8 protein coordinates EGF receptor signalling through Rac and trafficking through Rab5. Nature *408*, 374–377.

Liotta, L. A., and Kohn, E. (2004). Anoikis: cancer and the homeless cell. Nature *430*, 973–974.

Maffucci, T., Cooke, F. T., Foster, F. M., Traer, C. J., Fry, M. J., and Falasca, M. (2005). Class II phosphoinositide 3-kinase defines a novel signaling pathway in cell migration. J. Cell Biol. *169*, 789–799.

Malliri, A., Symons, M., Hennigan, R. F., Hurlstone, A. F., Lamb, R. F., Wheeler, T., and Ozanne, B. W. (1998). The transcription factor AP-1 is required for EGF-induced activation of rho-like GTPases, cytoskeletal rearrangements, motility, and in-vitro invasion of A431 cells. J. Cell Biol. *143*, 1987–1999.

Malliri, A., van Es, S., Huveneers, S., and Collard, J. G. (2004). The Rac exchange factor Tiam1 is required for the establishment and maintenance of cadherin-based adhesions. J. Biol. Chem. *279*, 30092–30098.

Moolenaar, W. H., van Meeteren, L. A., and Giepmans, B. N. (2004). The ins and outs of lysophosphatidic acid signaling. BioEssays *26*, 870–881.

Murga, C., Zohar, M., Teramoto, H., and Gutkind, J. S. (2002). Rac1 and RhoG promote cell survival by the activation of PI3K and Akt, independently of their ability to stimulate JNK and NF-kappaB. Oncogene *21*, 207–216.

Nakagawa, M., Fukata, M., Yamaga, M., Itoh, N., and Kaibuchi, K. (2001). Recruitment and activation of Rac1 by the formation of E-cadherin-mediated cell-cell adhesion sites. J. Cell Sci. *114*, 1829–1838.

Pankov, R., Endo, Y., Even-Ram, S., Araki, M., Clark, K., Cukierman, E., Matsumoto, K., and Yamada, K. M. (2005). A Rac switch regulates random versus directionally persistent cell migration. J. Cell Biol. *170*, 793–802.

Potempa, S., and Ridley, A. J. (1998). Activation of both MAP kinase and phosphatidylinositide 3-kinase by Ras is required for hepatocyte growth factor/scatter factor-induced adherens junction disassembly. Mol. Biol. Cell *8*, 2185–2200.

Reginato, M. J., Mills, K. R., Paulus, J. K., Lynch, D. K., Sgroi, D. C., Debnath, J., Muthuswamy, S. K., and Brugge, J. S. (2003). Integrins and EGFR coordinately regulate the pro-apoptotic protein Bim to prevent anoikis. Nat. Cell Biol. *5*, 733–740.

Rodrigues, G. A., Falasca, M., Zhang, Z., Ong, S. H., and Schlessinger, J. (2000). A novel positive feedback loop mediated by the docking protein Gab1 and phosphatidylinositol 3-kinase in epidermal growth factor receptor signaling. Mol. Cell Biol. *20*, 1448–1459.

Rodriguez-Viciana, P., Warne, P. H., Khwaja, A., Marte, B. M., Pappin, D., Das, P., Waterfield, M. D., Ridley, A., and Downward, J. (1997). Role of phosphoinositide 3-OH kinase in cell transformation and control of the actin cytoskeleton by Ras. Cell *89*, 457–467.

Sander, E. E., van Delft, S., ten Klooster, J. P., Reid, T., van der Kammen, R. A., Michiels, F., and Collard, J. G. (1998). Matrix-dependent Tiam1/Rac signaling in epithelial cells promotes either cell-cell adhesion or cell migration and is regulated by phosphatidylinositol 3-kinase. J. Cell Biol. *143*, 1385–1398.

Scita, G., Nordstrom, J., Carbone, R., Tenca, P., Giardina, G., Gutkind, S., Bjarnegard, M., Betsholtz, C., and Di Fiore, P. P. (1999). EPS8 and E3B1 transduce signals from Ras to Rac. Nature *401*, 290–293.

Scita, G., Tenca, P., Areces, L. B., Tocchetti, A., Frittoli, E., Giardina, G., Ponzanelli, I., Sini, P., Innocenti, M., and Di Fiore, P. P. (2001). An effector region in Eps8 is responsible for the activation of the Rac-specific GEF activity of Sos-1 and for the proper localization of the Rac-based actin-polymerizing machine. J. Cell Biol. *154*, 1–14.

Scita, G., Tenca, P., Frittoli, E., Tocchetti, A., Innocenti, M., Giardina, G., and Di Fiore, P. P. (2000). Signaling form Ras to Rac and beyond: not just a matter of GEFs. EMBO J. *19*, 2392–2398.

Sparatore, B., Patrone, M., Passalacqua, M., Pedrazzi, M., Ledda, S., Pontremoli, S., and Melloni, E. (2005). Activation of A431 human carcinoma cell motility by extracellular high-mobility group box 1 protein and epidermal growth factor stimuli. Biochem. J. *389*, 215–221.

Stradal, T., Courtney, K. D., Rottner, K., Hahne, P., Small, J. V., and Pendergast, A. M. (2001). The Abl interactor proteins localize to sites of actin polymerization at the tips of lamellipodia and filopodia. Curr. Biol. *11*, 891–895.

Tajima, K., Yoshii, K., Fukuda, S., Orisaka, M., Miyamoto, K., Amsterdam, A., and Kotsuji, F. (2005). Luteinizing hormone-induced extracellular-signal regulated kinase activation differently modulates progesterone and androstenedione production in bovine theca cells. Endocrinology *146*, 2903–2910.

Takaishi, K., Sasaki, T., Kotani, K., Nishioka, H., and Takai, Y. (1997). Regulation of cell-cell adhesion by Rac and Rho small G proteins in MDCK cells. J. Cell Biol. *139*, 1047–1059.

Van de Vijver, M. J., Kumar, R., and Mendelsohn, J. (1991). Ligand-induced activation of A431 cell epidermal growth factor receptors occurs primarily by an autocrine pathway that acts upon receptors on the surface rather than intracellularly. J. Biol. Chem. *266*, 7503–7508.

Vanhaesebroeck, B., Leevers, S. J., Ahmadi, K., Timms, J., Katso, R., Driscoll, P. C., Woscholski, R., Parker, P. J., and Waterfield, M. D. (2001). Synthesis and function of 3-phosphorylated inositol lipids. Annu. Rev. Biochem. *70*, 535–602.

Vasioukhin, V., Bauer, C., Mei, Y., and Fuchs, E. (2000). Directed actin polymerization is the driving force for epithelial cell-cell adhesion. Cell *100*, 209–219.

Vogelstein, B., and Kinzler, K. W. (2004). Cancer genes and the pathways they control. Nat. Med. *10*, 789–799.

Wang, Y. M., Seibenhener, M. L., Vandenplas, M. L., and Wooten, M. W. (1999). Atypical PKC zeta is activated by ceramide, resulting in coactivation of NF-kappaB/JNK kinase and cell survival. J. Neurosci. Res. *55*, 293–302.

Wheeler, M., and Domin, J. (2001). Recruitment of the Class II phosphoinositide 3-kinase C2β to the epidermal growth factor receptor: role of Grb2. Mol. Cell. Biol. *21*, 6660–6667.

Yaffe, M. B., Leparc, G. G., Lai, J., Obata, T., Volinia, S., and Cantley, L. C. (2001). A motif-based profile scanning approach for genome-wide prediction of signaling pathways. Nat. Biotechnol. *19*, 248–353.

Yamada, K. M., and Araki, M. (2001). Tumor suppressor PTEN: modulator of cell signaling, growth, migration and apoptosis. J. Cell Sci. *114*, 2375–2382.

Yamauchi, J., Miyamoto, Y., Tanoue, A., Shooter, E. M., and Chan, J. R. (2005). Ras activation of a Rac1 exchange factor, Tiam1, mediates neurotrophin-3-induced Schwann cell migration. Proc. Natl. Acad. Sci. USA *102*, 14889–14894.